

Sara Cristina Pardal Conceição

Bachelor degree in Biochemistry

Insights in dissimilatory sulfite reductase proteins

Dissertation to obtain the Master Degree in Biochemistry for
Health

Supervisor: Inês Cardoso Pereira, PI, ITQB-NOVA
Co-supervisor: Sofia Venceslau, PhD, ITQB-NOVA

March 2017

Sara Cristina Pardal Conceição

Bachelor degree in Biochemistry

Insights in dissimilatory sulfite reductase proteins

Dissertation to obtain the Master Degree in Biochemistry for
Health

Supervisor: Inês Cardoso Pereira, PI, ITQB-NOVA
Co-supervisor: Sofia Venceslau, PhD, ITQB-NOVA

Presidente do Júri:

– Doutor Pedro Matias, Investigador Principal do Instituto de Tecnologia Química e Biológica António Xavier da Universidade Nova de Lisboa;

Vogais:

– Doutora Margarida Archer (Investigadora Principal – Instituto de Tecnologia Química e Biológica António Xavier/UNL);

– Doutora Inês Cardoso Pereira (Investigadora Principal – Instituto de Tecnologia Química e Biológica António Xavier/UNL) – Supervisora

– Doutor José Artur Alves de Brito (Investigador do Instituto de Tecnologia Química e Biológica/UNL).

March 2017

Acknowledgements

First, I would like to thank my supervisors in this project Dr. Sofia Venceslau and Dr. Inês Pereira for receiving me in the laboratory, for taking the time to teach me the knowledge they have transmitted, for all the support during this thesis and for the guidance for the scientific work, and for the help in the reviewing of this thesis.

I also would like to acknowledge all of my lab partners in Bacterial Energy Metabolism group for always be available to help me, take your time to listen my questions and for teach me in all you were able to. Also for making such a great environment at work, to all the friendship that we have created.

To my work colleagues in Leroy Merlin Sintra for all the friendship, for help and understanding, for the good mood at every end of the day, you made my year much happier. A special thanks to Patricia Moreira for accepting me even with all the limitations of the time I had, and helping me to combine the master thesis with the work schedule.

To all my great friends, for being so understanding and caring, and even distant always find time to meet or talk with me. Specially to my greatest friends Catarina, Joana, Patricia, that always manage their times to see how I'm going, for sharing your good and bad moments with me, for all the great laughs and the many hours on the phone.

To all of my family, that was always there to support me, to for listen to me and for understanding my absence, and never forgetting about me. You are the most wonderful persons I know and I am so lucky that you are in my life, and as my family. A special thank you note to my grandparents that always show super excited with what I'm doing and for believing that I will really make a great difference in the world.

To my boyfriend Alexandre Neves, the most caring and loving person I know, that always stayed up late to talk to me while I was driving, for asking how was my work going and for always show excitement about the lab work, always asking "So how did the gels run today ?!". Even with so different schedules you where always there for me, and never gave up. You are amazing!

To my little sister, I hope to serve as a role model for you, I hope to teach you never give up on what you want even when things do not go as we expected, even when it's hard to never give up. I hope you always fight for your dreams and that I will always be by your side.

And at last but not least, the most important acknowledgement, to my parents, without you none of this had been possible, for all the guidance, support and funding. There is no way to thank you for everything you do for me, for supporting me in everything and for believing in me and my dreams, for always letting me choose my way and always stay by my side. There are no words to show how grateful I am for everything, and for the importance you have in my life. I hope one day to be as wonderful as you are.

Abstract

Microorganisms present in the gastrointestinal tract (GI) are essential in the digestion and production of enzymes for the degradation of otherwise indigestible polysaccharides. Some of the microorganisms present in the GI belong to the sulfate reducing bacteria group, which reduce sulfate to sulfide. These bacteria are also linked to inflammatory bowel diseases due to the toxic and corrosive effects of the sulfide produced.

The Dissimilatory sulfite reductase (DsrAB) is crucial for the reduction of sulfite, interacting with DsrC protein. DsrC is a protein that presents two conserved cysteines essential for the catalytic function. Another protein encoded in the same operon as DsrAB is DsrD, whose function is still unknown. In one organism, *Bilophila wadsworthia*, the *dsrD* gene is fused to *dsrB*. The main objective of this thesis was the study of these proteins, trying to understand the function of DsrD and the catalytic kinetic of DsrAB and DsrC.

In order to understand the function of DsrD, studies were carried out to evaluate the possible DsrD interaction with DNA through electrophoretic mobility shift assays, its interaction with other proteins through the Far Western Blot technique and interaction with possible substrates using Thermofluor assays. DsrABCD protein from *B. wadsworthia* was also purified and used for crystallographic and catalytic kinetic assays.

The DsrAB protein of *Desulfovibrio vulgaris* Hildenborough (*DvH*) was purified from a mutant strain so that it was possible to elute the DsrAB separately from DsrC, which is not possible in the wild-type species. DsrC from *DvH* was expressed and purified from *E. coli*, and sulfite reduction assays of DsrAB with DsrC were conducted.

Resumo

Os micro-organismos presentes no trato gastrointestinal são essenciais na digestão e na produção de enzimas para a degradação de polissacáridos que de outro modo seriam indigestíveis. Alguns dos micro-organismos presentes são as bactérias redutoras de sulfato, que utilizam o sulfato e o reduzem a sulfureto. Estas bactérias estão também ligadas à doença inflamatória intestinal.

A proteína reductase de sulfito dissimilativa (DsrAB) é crucial para este passo, interagindo com uma proteína, a DsrC, que apresenta cisteínas conservadas que estão envolvidas na ação catalítica. Outra proteína que se encontra no mesmo operão que a DsrAB é a DsrD, cuja função ainda é desconhecida. Num organismo em particular, *Bilophila Wadsworthia* o gene da *dsrD* encontra-se fundido com o da *dsrB*. O objetivo principal desta tese foi o estudo destas proteínas, tentando entender a função da DsrD e a cinética catalítica da DsrAB e DsrC.

Para entender a função da DsrD foram feitos estudos para a interação com DNA através de ensaios de deslocamento de mobilidade eletroforética; outras proteínas através da técnica de Far-Western Blot; e com possíveis substratos em ensaios de Termofluor. A proteína DsrABCD de *Bilophila* foi também purificada e utilizada para ensaios cristalográficos e cinéticos.

A proteína DsrAB de *Desulfovibrio vulgaris* Hildenborough foi purificada através de um mutante de modo a que fosse possível a eluição da DsrAB sem DsrC, que não é possível na espécie *wild-type*. A DsrC de *DvH* foi expressa e purificada em *E.coli*, e a cinética da adição desta proteína à DsrAB foi analisada.

Content Index

Acknowledgements.....	iii
Abstract	v
Resumo.....	vii
Content Index.....	ix
Figure Index.....	xi
Tables index.....	xiii
List of abbreviations	xv
I. Introduction	1
Gut Microbiome	1
Inflammatory Bowel Disease	2
Sulfur	3
Respiratory chain	6
Close up view of the DSR proteins	7
II. Methods	13
Purification of DsrD	13
Western Blot optimization process.....	13
Electrophoretic mobility shift assay (EMSA)	14
Thermofluor assay.....	15
DsrD Expression Differences	15
Far Western Blot	16
Purification of <i>Bilophila wadsworthia</i> DsrABC	16
Kinetic Studies	17
Purification of DsrAB from IPFG07 strain.....	17
Purification of DsrC	18
Kinetic assays	19

III. Results and discussion.....	21
Characterization of DsrD	21
<i>Bilophila wadsworthia</i>	29
DsrAB from IPFG07 and DsrC_C26A.....	35
IV. Conclusions	39
V. Bibliography	41
Supplementary Data	45

Figure Index

Figure I.1 - Microbiome composition in different stages of life [9].	1
Figure I.2 – Factors that impact IBD's.	3
Figure I.3 - Biological sulfur cycle. Adapted from [20].	4
Figure I.4 - Sulfate reduction mechanism. Described in [17], [35].	7
Figure I.5 - Crystallographic structure of DsrAB co-crystallized with DsrC. In green it shows DsrA, in blue DsrB and in orange DsrC. Adapted from [37].	8
Figure I.6 - Last step of sulfite reduction. a) siroheme receives electrons and transfer them to sulfite, forming an intermediate that binds do the nearby cysteine in C-terminal (in blue); B) trisulfide state, where the sulfur from sulfite is bound to the two cysteines. From the ITQBNOVAchannel (2015) https://www.youtube.com/watch?feature=player_embedded&v=NOMG7SrFKyw (viewed Feb 2017).	9
Figure I.7 - Sequence alignment of DsrBD from <i>B. wadsworthia</i> and DsrB & DsrD from <i>DvH</i> .	10
Figure I.8 - Dimeric structure of DsrD. B-sheets in green, a helix in red and disordered regions in blue. Adapted from [43].	11
Figure II.1 – Purification of DsrABC from <i>Bilophila wadsworthia</i>	17
Figure III.1 - Purification of DsrD. A) Tricine-SDS-PAGE; MW- molecular mass markers (kDa); 1- First fraction eluted at 100 mM of imidazole; 2- Second fraction eluted at 500 mM of imidazole; 3- First fraction in non-reductive conditions (5 µg of protein). B) UV-Vis spectra of DsrD.	21
Figure III.2 - Western blot optimization results. MW - Molecular weight (kDa); WT - wild type <i>DvH</i> ; ΔD - <i>DvH</i> mutant without <i>dsrD</i> gene; BB - lysed with Bug Buster; LM - lysed by mechanical lysis, with MiniLys; 40 and 80 µg of total protein extract was used.	22
Figure III.3 - Growth curves of <i>DvH</i> with different electron acceptors: Sulfate, sulfite, and thiosulfate.	24
Figure III.4 – DsrD expression in different growth conditions. MW – Molecular weight marker; 1, 2, 3 - samples taken at mid-point exponential phase from sulfate, sulfite, and thiosulfate grown <i>DvH</i> cells, respectively; 4, 5, 6 - samples taken at the end of exponential phase from sulfate, sulfite, and thiosulfate grown <i>DvH</i> cells, respectively.	24
Figure III.5 - Electrophoretic mobility shift assay. A) schematic representation of the assay, with free and bound DNA; B) example of the results obtained, MW - DNA markers, C - DNA with	

no protein; 1-5 DNA incubated with increasing concentration of protein from 100 to 500 pmol of protein.	25
Figure III.6 - Far Western Blot Results. A) membrane incubated with DsrD protein; B) Control membrane, without incubation; 1 – DsrAB, 2 - DsrMKJOP, 3 – DsrC , 4 - DsrD.....	27
Figure III.7 - Purification summary. A) Tricine-SDS PAGE gel. B) Native gel; in A and B panels lane 1- fraction after the chromatographic step; lane 2 - fraction 1.1 after the electro elution purification step; lane 3 - DvH DsrABC. C) UV-vis spectrum of purified DsrABDC from <i>B. wadsworthia</i>	30
Figure III.8 – Activity versus concentration of protein. Assays performed at 35 °C with sulfite concentration of 500 µM. In blue dots are the results for the first batch #1.1 and in orange squares the results for the second batch #2.1.....	31
Figure III.9 - Activity versus sulfite concentration at 35 °C. In blue dots are the results for #2.1 with the protein concentration of 25 nM.	32
Figure III.10 - Crystal of DsrABDC protein, from the screening of crystallographic conditions. .	34
Figure III.11 - Purification of DsrAB from the IPFG07 mutant. A) Chromatogram of HiTrap IMAC affinity column. 1 to 6 represents the fractions obtained from the elution with increasing steps of imidazole. B) Western blot against DsrC with the fractions from the chromatogram (30 µg of protein). C) SDS-Page of DsrAB, 1 – DsrAB from IPFG07.	36
Figure III.12 – A) Kinetic results from the addition of <i>DvH</i> DsrC to DsrAB enzyme; B) Kinetic profile from the addition of <i>A.fulgidus</i> DsrC to DsrAB in sulfite reduction,taken from [35].....	37
Figure III.13 - MalPEG assay; on the left panel reduced DsrC incubated (+) and non-incubated (-) with MalPEG; on the middle panel DsrC with DsrAB and sulfite non incubated (-) and incubated (+)with MalPEG in different time points during the kinetic assay, from 0 to 15 minutrs (+T); on the right panel reduced DsrC after the addition of sulfite incubated (+) and non-incubated (-) with MalPEG.....	38
Figure S.1 – Chromatogram from Q-Sepharose column for the purification of DsrABDC from <i>Bilophila wadsworthia</i>	42
Figure S.2 – Chromatogram from Q-Sepharose column for the purification of DsrABC from <i>DvH</i>	43

Tables index

Table I.1 – EMSA conditions tested.....	14
Table III.2 – Melting temperatures in the different conditions tested. The results shown are the average of triplicates.....	26
Table III.3 – Concentrations obtained in both batches of the purification in the two main fractions containing DsrABDC.	29
Table III.4 – Hyper 32 fitting results for Hyperbolic Regression, and the hyperbola graph obtained.	32
Table III.5 – Summary table for the kinetic parameters for Dissimilatory sulfite reductases from different organisms.....	33
Table S.1 – Growth medium for <i>Desulfovibrio vulgaris</i> Hildenborough.....	42

List of abbreviations

ATP – Adenosine Triphosphate

B. Wadsworthia – *Bilophila Wadsworthia*

DvH – *Desulfovibrio Vulgaris* Hildenborough

Dsr – Dissimilatory Sulfite Reductase

GI– Gastrointestinal Tract

MalPEG - Methoxypolyethylene Glycol Maleimide

PAGE – Polyacrylamide Gel Electrophoresis

PVDF – Polyvinylidene Difluoride

QMO – Quinone Interacting Membrane Oxidoreductase Complex

SCFA – Short Chain Fatty Acids

SDS – Sodium Dodecyl Sulfate

SOO – Sulfur Oxidizing Organism

SRB – Sulfate Reducing Bacteria

SRO – Sulfate Reducing Organism

HEPES – *4-(2-Hydroxyethyl)-1-Piperazineethanesulfonic Acid*

I. Introduction

Gut Microbiome

The gut microbiome plays a key role in metabolic, physiological, nutritional and immunological processes, therefore it is directly related to human health [1][2]. At the time of birth, the human body is sterile and starts to be colonized during labor, which continues throughout life, through multiple ways like the air, food and others. Multiple factors influence the microbiota, for example, some studies report that the microbiome is different in infants born vaginally or by caesarean, and also in children fed by breastfeeding or formula [3–5].

In the human gastrointestinal (GI) there are about 10^{14} microorganisms, found in six major sections: oral cavity, esophagus, stomach, small intestine, the colon and the rectum [6]. The different sections have different floras, and each person has a different microbiota composition, there is, however, a core group present in the great majority of individuals [7]. The most prevalent organisms found in the adult human gut are members of the *Firmicutes* and *Bacteroidetes* phyla. Other phyla as *Proteobacteria*, *Actinobacteria*, *Fusobacteria*, and *Verrucomicrobia* are also present, although in a smaller dominance (figure I.1) [8][9].

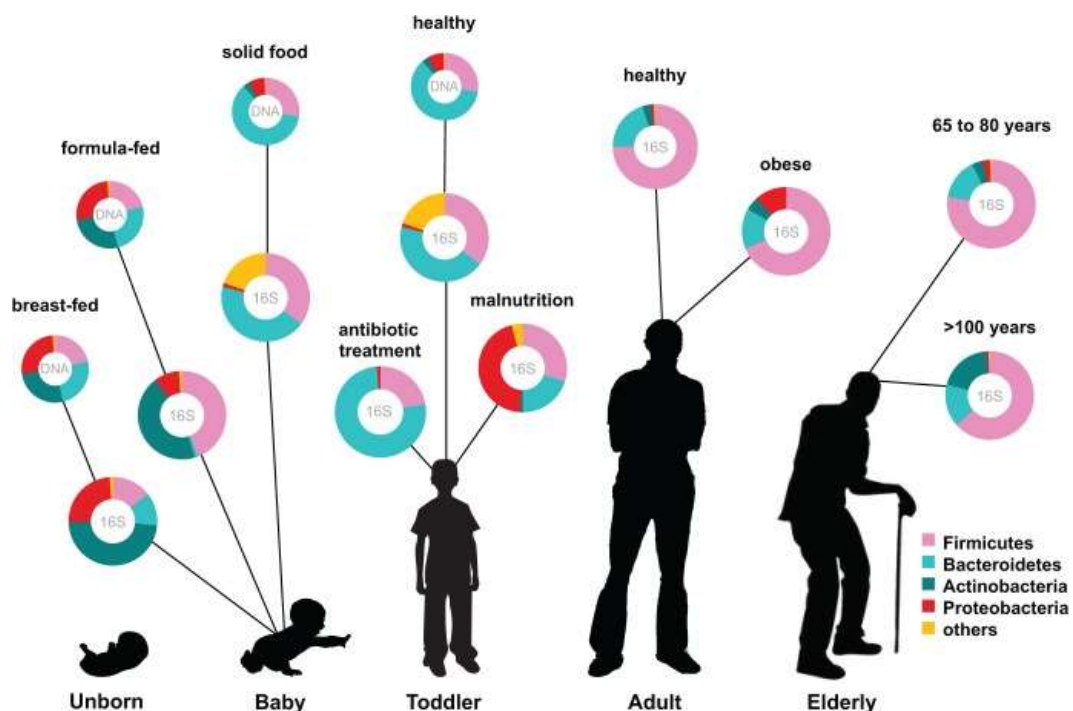


Figure I.1 - Microbiome composition in different stages of life [9].

An important function of the intestinal flora is to increase the genetic repertoire. The intestinal microbiota makes possible the degradation of dietary fibers and complex polysaccharides, otherwise indigestible by endogenous enzymes [10]. Anaerobic microorganisms present in the intestine have the ability to degrade complex carbohydrates into monosaccharides, which can be assimilated or fermented. The main products of gut fermentations are short-chain fatty acids (SCFA) and hydrogen sulfide (H₂S). SCFAs are saturated aliphatic organic acids that consist of one to six carbons, easily metabolized and essential for energy production [11]. The microbiota is also involved in vitamin biosynthesis, degradation of amino acids, catabolism of simple sugars, and bile salt metabolism, making this symbiosis with microorganisms essential [9, 12]. These bacteria also provide protection against pathogens and maintain homeostasis that is important for differentiation of the epithelium and the modulation of the immune system.

Microbial diversity will change along time with some factors such as age, diet, environment, antibiotics and diseases, among others. Studies about the microbiome are becoming increasingly important in the past few years (with the development of high-throughput techniques for genome sequencing), aiming to understand the mechanisms that promote microbial symbiosis and a causal relationship with diseases, like Inflammatory Bowel Diseases (IBD's) [1].

Inflammatory Bowel Diseases

Inflammatory bowel diseases are characterized by a chronic, relapsing inflammation in the GI tract, caused by a microbial imbalance (dysbiosis) of the host-commensal microbiota that leads to a dysregulation of the immune tolerance to these commensal microbes, especially in genetically predisposed hosts. It is regarded be as a multifactorial disease involving several factors such as genetic, physiological, bacterial, environmental and even diet (figure I.2). The IBD's are mainly divided into two diseases, Crohn's Disease (CD) and Ulcerative Colitis (UC), that present different pathogenesis, inflammatory profiles and gut microbiota composition [13].

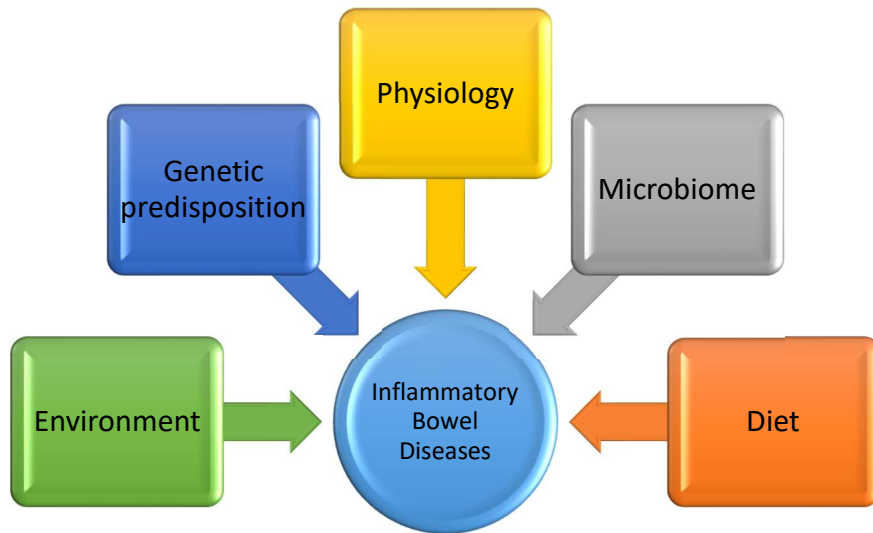


Figure 1.2 – Factors that impact IBD's.

Although similar, there are differences between these two diseases. The UC disease is mainly limited to the colon in the superficial mucosa, while CD can be present in the entire human gut, is transmural and can present granulomas [14]. The cytokine profile between the two conditions is also different. CD is mostly related with type 1 helper-T-cell (Th1) and type 17 helper-T-cell (Th17) immune responses, characterized by increased production of interleukin (IL)-12, IL-23, IL-27, interferon- γ (IFN- γ) and tumor necrosis factor (TNF)- α . On the other hand, UC is related to a type 2 helper-T cell (Th2) immune response, mainly leading to raised levels of IL-5 and transforming growth factor- β (TGF- β) [15]. The principal clinical features of CD include persistent diarrhea, crampy abdominal pain, fever, occasional rectal bleeding and fatigue, while the main symptoms of UC include crampy abdominal pain, loose and bloody stools, urgent bowel, fatigue, loss of appetite, and in severe cases anemia due to blood loss.

IBD's are not the only condition caused by this dysbiosis. Over the past years, it's been linked to a number of extraintestinal immune-mediated diseases including rheumatoid arthritis, multiple sclerosis, diabetes, atopic dermatitis, and asthma, but also obesity and metabolic syndrome, all of which could well have their pathogenic origins an untoward reactivity of the immune system to the microbiota [16].

Sulfur

Sulfur is the sixth most abundant element on Earth. It is being involved in many biological and geophysical processes and it is present in many diverse molecules from amino acids to

minerals. Sulfur has a broad range of oxidation states, from -2 (fully reduced) in H_2S , to +6 (fully oxidized) in SO_4^{2-} , and can be transformed both chemically and biologically. The oxidation is performed chemically or by sulfur oxidizing microorganisms and transforms the sulfur to sulfate. The reduction is more common in bacteria or fungi and reduces sulfate (SO_4^{2-}) to sulfide (S^{2-}) [17, 18].

The microorganisms play an essential role in the interconversion of the redox states of sulfur (figure 1.3), interacting as sulfate reducing organisms (SRO) or sulfate oxidizing organisms (SOO). This thesis will focus on SRO, where sulfur compounds can follow two pathways. The assimilatory pathway, in which sulfate is reduced to be used to integrate amino acids such as cysteine and other small biological sulfur-containing molecules - like protein co-factors, nucleosides, vitamins, and co-enzymes - or the dissimilatory pathway in which sulfate will be utilized as the terminal electron acceptor for the production of energy. Many organisms have the ability to metabolize sulfate by the assimilatory pathway, but only a few groups of microorganisms can reduce sulfate dissimilatively [19].

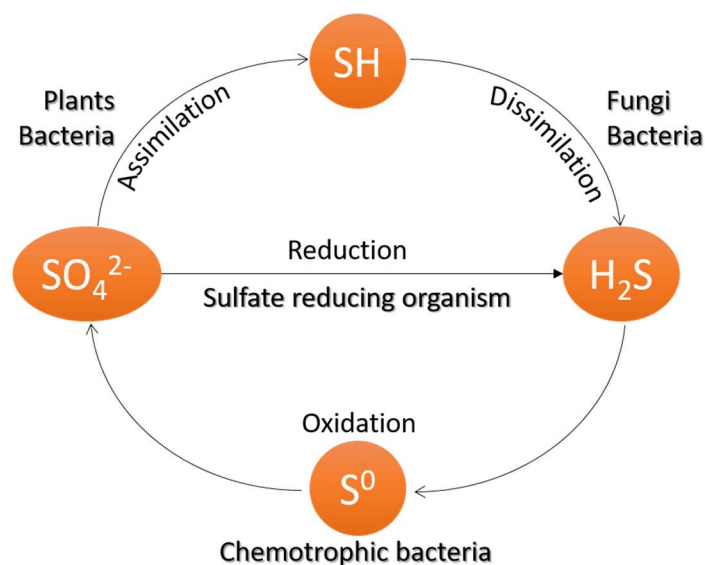


Figure 1.3 - Biological sulfur cycle. Adapted from [20].

In the phylogenetic tree, SRO can be found in the *Bacteria* and *Archea* kingdoms. They can be found in very diverse environments such as seawater, mud volcanoes, hydrothermal vents, and human gut, among others. They are also present in habitats with a wide range of pH and even at saturating oxygen concentrations [20]. The use of sulfur compounds in cellular

metabolism dates back to the time when Earth was an anoxic planet, with major volcanic activity where many sulfur compounds were released to the atmosphere. Since there was no oxygen present, the development of a great diversity of mechanisms for energy production occurred, such as a reduction of sulfur-based products. With the rise of oxygen levels on the planet, the levels of sulfate in the ocean became higher (up to 28 mM nowadays), leading to an increase of SRO in the suboxic and anoxic zones of marine sediments [19].

The wide distribution of sulfate reducing organisms in the environment leads to multiple biotechnology problems. One of them is the bio-corrosion of ferrous metals, leading to the damage of pipes and corrosion of metal structures. Also in many industrial processes where sulfuric acid is used, the occurrence of sulfate in wastewaters where SRO are present, creating sulfide which is highly toxic and corrosive [21]. On the other hand, sulfate reduction can be useful for biotechnology, such as in the removal of heavy metals from waste waters or contaminated soils by precipitation as metal sulfides [20]. There are new methodologies for the removal of pharmaceutical products using metals and sulfate-reducing bacteria (SRB), proving that SRO can be useful also in the bioremediation of organic compounds [22].

Another place where SRB are can have beneficial and detrimental effects is the human gut. There are some bacteria believed to be directly involved in the development of IBD, namely sulfate-reducing bacteria (SRB). Although SRB are not always present in the fecal matter they are always present in the intestinal mucosa [23]. The groups of SBR present in the gut belong to the *Desulfovibrio*, *Desulfobacter*, *Desulfobulbus* and *Desulfotomaculum* genus, but the most predominant belong to *Desulfovibrio* genus, approximately 66% of all colonic SRB. These species have the ability to use H₂ or carbon sources like SCFA or as electron donors and SO₄⁻ as an electron acceptor in the electron transport chain. A major problem in human health is that the end product of this respiration is hydrogen sulfide (H₂S), a gas with the characteristic odor of rotten eggs that is toxic and corrosive, and can cause major inflammation in the bowel, being appointed as one of the factors that lead to inflammatory bowel diseases, described above.

Although it can cause health problems, several studies recognize H₂S as an important gaseous signaling molecule, playing an important role in human physiology. When present in lower levels it is proven to have beneficial physiological effects, like regulation of vasorelaxation, regulation of the cellular cycle and apoptosis, cellular energy production, neuromodulation of inflammatory processes, among others, but at higher concentrations it can cause detrimental effects [24]. However, the mechanism of H₂S action in IBD is not well known, and the unraveling of this problem would be very useful for human health.

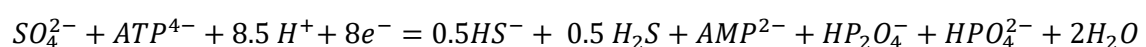
The main electron acceptor for SRO is sulfate, although usually they can also use other sulfur compounds, such as thiosulfate, sulfite or organosulfonate compounds. The carbon compounds suffer an incomplete oxidation to acetate by SBR species like *Desulfovibrio* [25, 26]. *Desulfovibrio vulgaris* Hildenborough (DvH) is a model organism to study the energy metabolism of SRB, and was the first SRB to have its genome sequenced [27]. DvH is a Gram-negative, anaerobic, non-spore forming, curved rod-shaped bacteria, that belongs to the *Desulfovibrionaceae* family. It has many unique periplasmic heme-containing proteins, like cytochrome c_3 , that allow adaptive strategies [28]. It can use SCFA like lactate, pyruvate, formate, as carbon source and sulfate and sulfur intermediates in the electron transfer chain [27].

The organism *Bilophila wadsworthia* is another gram negative bacterium, strictly anaerobic, a member of the human gut flora and occasionally found in saliva and in some infections, being identified many times in appendicitis [29]. Its handling in the laboratory must be done with care presenting a Biosafety level 2 given its clinical relevance. This organism uses taurine as the electron acceptor, which is metabolized into sulfite, that is then reduced by dissimilatory sulfite reductase (Dsr) proteins. However, it does not reduce sulfate, and it can also grow using hydrogen [30].

Respiratory chain

Sulfate is a very stable molecule, and it's not easy to change it. For that reason, the reduction of sulfate first requires its activation because the SO_4^{2-} anion is very stable and its reduction has a very low redox potential (-526 mV). The first step is performed by sulfate adenylyltransferase (SAT), that uses ATP to catalyze the production of adenosine phosphosulfate (APS) and pyrophosphate, which will subsequently be hydrolyzed to 2-phosphate, by pyrophosphatase.

Two electrons are used by APS reductase to reduce APS to sulfite. In the next step it was thought that bisulfite reductase (DsrAB) used six electrons to reduce HSO_3^- to S^{2-} - that can also be present as H_2S , depending on the pH - in a single step. The complete reaction of sulfate reduction requires one ATP molecule and 8 electrons (equation 1) [31].



Equation 1 – Sulfate reduction summary. Adapted from [31]

Where do the electrons come from? The proposed mechanism describes the membrane complex QmoABC as the physiological partner of APS reductase [32]. The APS reductase protein binds FAD as a cofactor and receives electrons from the Qmo complex. These electrons are supposed to come from the quinone pool, in the membrane, and ferredoxin, in the cytoplasm [33]. Some studies have been carried out to understand the role of this complex, and mutants of *Desulfovibrio vulgaris* showed that when lacking the *qmo* genes, *DvH* can grow from sulfite or thiosulfate, but not from sulfate, showing that the complex is essential for the activation of sulfate to APS [34].

For the reduction of SO_3^{2-} , the dissimilatory sulfite reductase (DsrAB) protein receives electrons from the membrane complex DsrMKJOP [32], with the help of DsrC, a protein that works as a co-substrate for the DsrAB [35] (figure I.4). The Dsr proteins are enzymes essential for the sulfur cycle, are extremely well conserved in SRO, and are also present in many SOO.

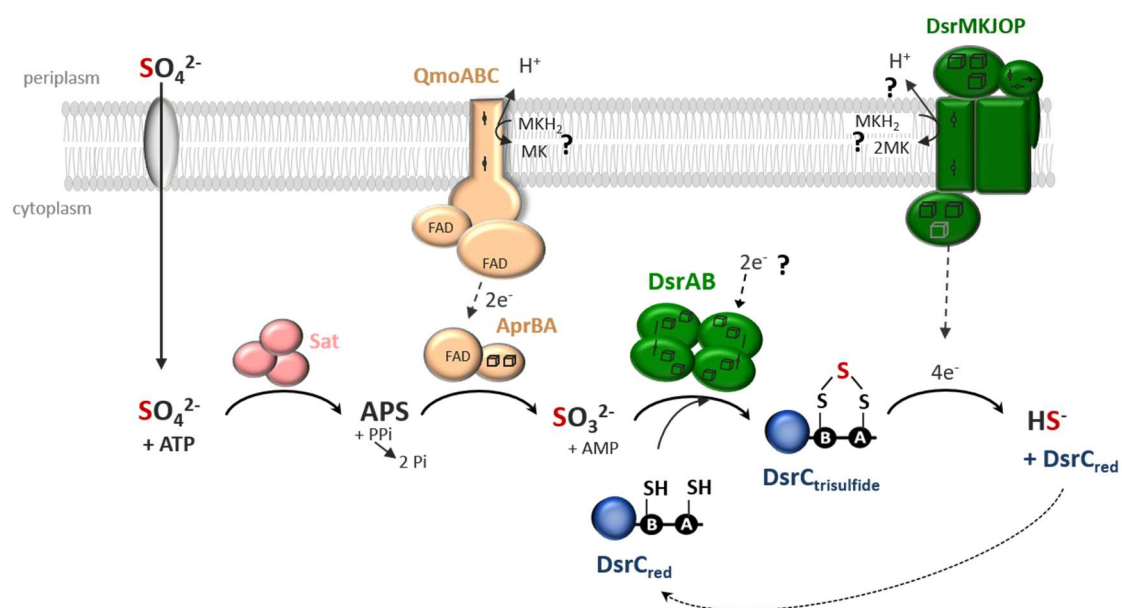


Figure I.4 - Sulfate reduction mechanism. Adapted from [17, 35]

Close up view of the DSR proteins

For the reduction of sulfite, there are three major proteins involved, DsrAB, DsrC and a membrane complex, DsrMKJOP. DsrAB is called dissimilatory sulfite reductase, a protein of approximately 200 kDa with a green color and two sub-units, DsrA and DsrB, in a $\alpha_2\beta_2$

arrangement (figure I.5). This enzyme contains two siroheme cofactors in each $\alpha\beta$ unit, one of which is coupled to a [4Fe – 4S] cluster through the cysteine heme axial ligand [36][37].

The *dsrA* and *dsrB* genes are very similar and it is proposed that they are derived from a gene duplication event followed by a gene fusion. These genes are present not only in SRO but also in sulfate oxidizing bacteria, and organisms that reduce sulfite, thiosulfate, and other organosulfonates. The DsrAB are classified based on their UV-Visible absorption characteristic. The characteristic absorption peak in our studies is at 630nm, observed in *Desulfovibrio* strains.

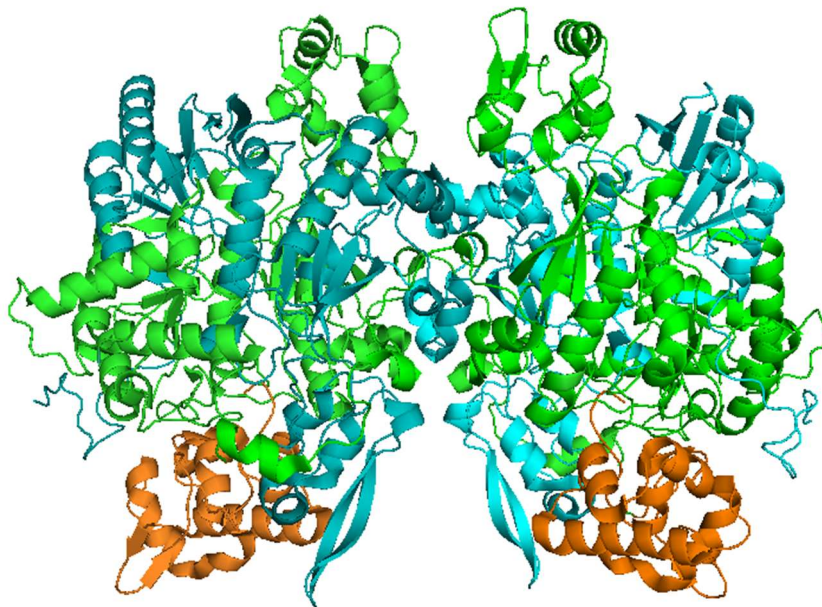


Figure I.5 - Crystallographic structure of DsrAB co-crystallized with DsrC. DsrA is shown in green, DsrB in blue and DsrC in orange. Adapted from [37].

Another essential protein for sulfite reduction is DsrC, a small protein with approximately 14 kDa, that is isolated from *Desulfovibrio* along with DsrAB, forming a complex $\alpha_2\beta_2\gamma_2$ [38]. All of the genomes containing the *dsrAB* genes also encode *dsrC*, it is one of the most expressed genes and this protein presents two conserved cysteines in the C-terminal[39]. These cysteines are present in a flexible arm that inserts into the DsrAB catalytic cavity, extending towards the siroheme, and being involved in the catalytic process.

The role of DsrC has recently been unveiled. The studies were made in *Archaeoglobus fulgidus*, an organism where DsrAB and DsrC can be isolated separately. The new evidence showed that DsrC is a co-substrate for DsrAB in sulfite reduction. DsrC provides two electrons

for sulfite reduction by DsrAB. The extended arm inserts to the catalytic center. The siroheme receives electrons and binds to sulfite that gets reduced, and finally the sulfur binds to DsrC through the conserved cysteines, forming a trisulfide (figure I.6) [35].

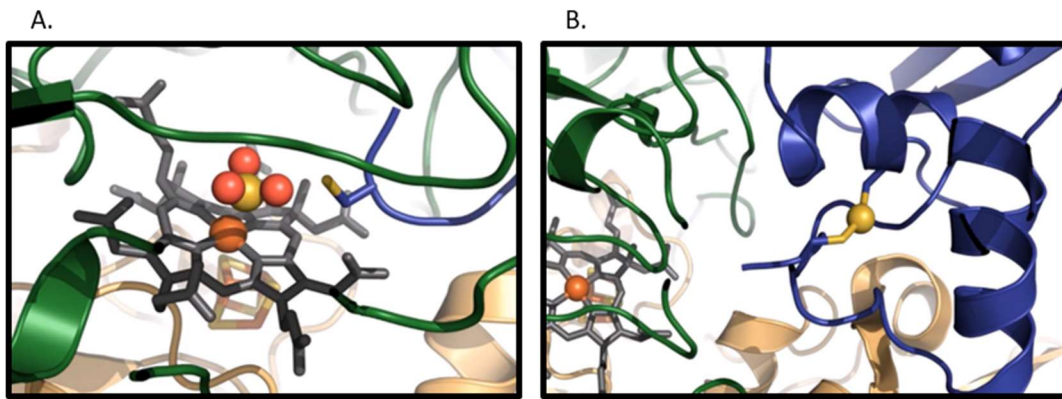


Figure I.6 - final step of sulfite reduction. a) The siroheme receives electrons and transfer them to sulfite, forming an intermediate that binds to the nearby cysteine in the C-terminal (in blue); B) trisulfide state, where the sulfur from sulfite is bound to the two cysteines. From the *ITQBNOVAchannel* (2015) https://www.youtube.com/watch?feature=player_embedded&v=NOMG7SrFKyw (viewed Feb 2017)

DsrD from *DvH* is a small protein with 78 amino acids and a molecular weight of approximately 8.8 kDa [40]. The *dsrD* gene is found downstream of the *dsrAB* genes. The DsrD protein also seems to be highly conserved across the SRO, being present in Gram negative bacteria - as *Desulfovibrio* - and Gram positive bacteria, and also in archaea, as *Archaeoglobus* spp., showing that it is an important component of the sulfite reduction mechanism [40]. The genome of *B. wadsworthia* has shown a particularity in the *dsr* genes, where instead of *dsrD* being present downstream from the *dsrB* gene, they are merged forming a DsrB-DsrD protein (figure I.7), suggesting a direct involvement of DsrD in sulfite reduction, and making it a protein of interest for the unveiling of this mechanism [41].

```

      *           20           *           40           *           60           *
BW_DsrBD : MAFVSSGYNPEKPMEGRISDIGPRKYDSFFPEV IKNFGKWLYHEILEPGVL VHVAESGDKVYTVRCGGTRTM : 73
DvH_DsrB : MAFI SSGYNPEKPMANRITDIGPRKFDFFPPVIANKFGSWLYHEILEPGVLMHVAESGDKVYTVRVGAARLM : 73
      80           *           100          *           120          *           140
BW_DsrBD : SVTNIRE I CEIADKYCDGHWRTTRNNIEFMVTDEATLKALKEDLAGRKFAAGSYKFPPIGGTGAGVSNIVHTQ : 146
DvH_DsrB : S I THIREMCDIADKYCGGHLRFTTRNNVEFMVADEASLKALKEDLASRKFDGGSLKFPPIGGTGAGVSNIVHTQ : 146
      *           160          *           180          *           200          *           140
BW_DsrBD : GWVHCHTPATDASGPKAVMDT MFEFKNMRLPAPVRISLACCINMCGAVHCSDIGIVGIHRKPPMIDDQWVD : 219
DvH_DsrB : GWVHCHTPATDASGPKA IMDEVFEDFQSMRLPAPVRISLACCINMCGAVHCSDIGVVGVIHRKPPMIDHEWTD : 219
      220          *           240          *           260          *           280          *
BW_DsrBD : QLCEIPLAVAACPAAVRPVKSEHDGKKNVSAIKQDRCMYCGNCTMCPALPISDGEGDGIALMVGKVSNR : 292
DvH_DsrB : QLCEIPLAVASCPAAVRPTKLE IGDKKVNT IA IKNERCMYCGNCTMCPALPISDGEGDGVVIMVGKVSNR : 292
      300          *           320          *           340          *           360
BW_DsrBD : ISMPKFSKVVVAYIPNEPPRWNTLTSTIKHIVEVYSENANKYERLGDWAERIGWESFFELTGLEFTHHLIDDF : 365
DvH_DsrB : ISMPKFSKVVVAYIPNEPPRWPSLTKTIKH I EVYSANAYKYERLGEWAERIGWERFFSLTGLEFSHHLIDDF : 365
      *           380          *           400          *           420          *
BW_DsrBD : RDPAYYTWQRSTQKFSELAALAAHGGEAHEAASAEVTAEDKEIVNFLKDKMSRPGAKTKYFKDFLELFPA : 438
DvH_DsrB : RDPAYYTWQRSTQKFF----- : 381
DvH_DsrD : -----MEEAKQKVDFLN---SKSGSKSKFYFNDFTDLFPD : 33
      440          *           460          *           480          *           420          *
BW_DsrBD : KGTRDVKNVLSVLVSEESLEYWSSGSTMVYGLKGAGKQASSEGEN : 483
DvH_DsrD : MKQREVKKILTALVNDEVLEYWSSGSTMVYGLKGAGKQAAAEHED : 78

```

Figure I.7 - Sequence alignment of DsrBD from *B. wadsworthia* and DsrB & DsrD from *DvH*.

The actual function of the DsrD protein remains unknown. In the amino acid sequence of this protein there is no cysteine or cofactors, which makes electron transfer with this protein unlikely. However, it has a high content of lysines (11.8%). A possible explanation for the high content of this positively charged amino acid was that perhaps DsrD has an anion binding protein function, binding the sulfite or sulfide in the cell, so that it is not be toxic for the cell. However, spectroscopic studies showed that DsrD has low affinity for these sulfurated compounds, less than 10^{-4}M^{-1} [42].

Crystallographic structure of DsrD (figure I.8) has a winged helix motif, a sub family of the helix-turn-helix motifs (structural motifs for DNA binding). This motif is composed of three α helix and three β strands forming an antiparallel β sheet. The protein forms a dimeric assembly in the crystal, but in solution there is no indication of a dimeric form. In the structure there is a hydrophobic core formed by hydrophobic residues [43].

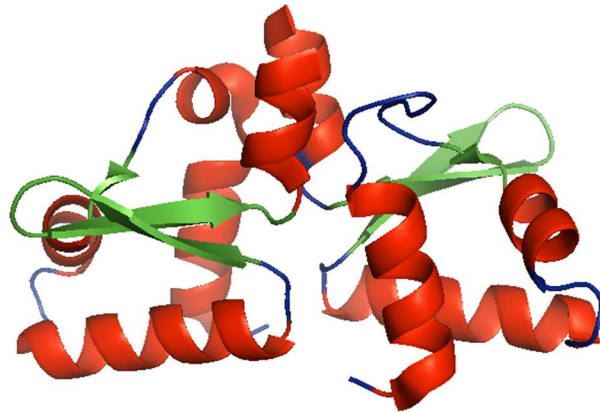


Figure I.8 - Dimeric structure of DsrD. B-sheets in green, a helix in red and disordered regions in blue. Adapted from [43]

The structural evidence, the structural homology with proteins with known functions [44], and the fact that in most SRB DsrD is expressed alone and not as a fusion protein, leads to the hypothesis that the protein interacts with B-DNA or Z-DNA, and is involved in transcriptional regulation. The lack of evidence evidence that DsrD binds sulfate, sulfite or sulfide (only binds with low affinity on the protein surface), and the presence of a winged helix motif, with a hydrophobic core, suggests a possible function as a regulatory protein.

Some studies have shown that although DsrD is in the same operon as DsrAB, it does not co-purified with them, although it is constitutively expressed in *D. vulgaris* [42]. The aim of this thesis is to investigate the function of this protein in sulfate reduction, namely its possible role as a regulator.

II. Methods

Purification of DsrD

In previous work the *DvH dsrD* gene was cloned into pET_{-22b(+)} vector (Novagen®), which allows insertion of a 6x-His tag at the C-terminus. Then the recombinant plasmid was transformed in to *E. coli* BL21-Gold(DE3) and grown at 37 °C in M9 minimal medium with ampicillin (100 µg/mL), until optical density of 0.4. Then, 100 µM isopropyl-β-D-thiogalactopyranoside (IPTG) was added to induce expression and cells were grown for 4 additional hours.

After centrifugation, the cells were resuspended in 25 mM potassium phosphate, 300 mM NaCl, 30 mM imidazole and 10% glycerol pH 7.2 (buffer A), and then disrupted through mechanical lysis with glass beads (~100 µm) in a Minilys (Bertin technologies), and subsequently centrifuged at 13.300 rpm for 20 minutes. The supernatant was filtered and loaded into a HiTrap Column charged with nickel and equilibrated with buffer A, and then it was eluted with the same buffer plus 100 mM imidazole. The protein was dialyzed to 25 mM potassium phosphate pH 7.2 and the purity was analyzed by SDS-PAGE. The concentration was determined at 280 nm using absorption coefficient of 9.9 mM⁻¹ cm⁻¹. This protein was used to perform multiple studies with the aim to find its biological role.

Western Blot optimization process

DvH wild-type and a deletion mutant strain, where the *dsrD* gene was replaced by a kanamycin resistance cassette, were grown in anaerobic conditions in a rich medium with 60 mM Pyruvate, 3 mM sulfate and geneticin (100 µg/mL), until an optical density of approximately 0.5 was reached. The cells were harvested by centrifugation and treated with two different lysis protocols. One batch of cells were resuspended in Bug Buster Protein Extraction Reagent (Novagen®) and another batch was resuspended in 50 mM potassium phosphate pH 7.4, 10% glycerol and protease inhibitor cocktail, and lysed in a Minilys. The resulting extracts were centrifuged at 13.300 rpm for 15 minutes to remove cell debris. The soluble crude extracts were quantified with a Bradford assay and 40 µg of each protein sample were subject to 10% Tricine-SDS-PAGE, that were transferred to 0.22 µm PDVF membrane (polyvinylidene difluoride) membranes (Roche) at 100 V in a Mini Trans-Blot wet cell (Bio-Rad) for 6 to 8 minutes (transfer buffer: 48 mM Tris and 39 mM Glycine pH 9.2). This process was repeated multiple times and multiple different were tested for the detection.

The membranes were dried overnight and then blocked with TBS (20 mM Tris-HCl pH 7.5, 150 mM NaCl) containing 5% dry milk. Western blot analysis was conducted using the primary antibody anti-DsrD from *DvH* (DsrD antiserum, in different dilutions: 1:5.000; 1:10.000; 1:20.000) for 1 hour in TBST (TBS with 0.05% Tween 20), followed by incubation with the secondary antibody, anti-rabbit IgG conjugated with alkaline phosphatase (1:15.000, Sigma). The protein detection was performed with Alkaline Phosphatase Buffer (100 mM Tris-HCl pH 9.5, 100 mM NaCl and 5 mM MgCl₂) and substrate solution of nitro-blue tetrazolium and 5-bromo-4-chloro-3'-indolyphosphate (NBT/BCIP).

Electrophoretic mobility shift assay (EMSA)

The DNA-Protein interaction was tested with an electrophoretic mobility shift assay [45, 46]. The promotor region of *dsrAB* genes was amplified using synthetic primers and the *DvH* genomic DNA as template. PCR fragments were purified with agarose gel extraction kit (Thermofisher). The DNA was incubated with DsrD or DsrC proteins in multiple conditions, as described in table I.1

Table I.1 – EMSA conditions tested.

Incubation	Binding Buffer: 20 mM Tris-HCl pH 8 + 10% glycerol + 1 mM MgCl ₂ + 40 mM KCl 25 minutes at 37 °C
	Binding Buffer: 5 mM HEPES pH 7.8 + 20 mM KCl + 0.02% Tween 20 + 1 mM TCEP 15 minutes at room temperature
	Binding Buffer: 5 mM HEPES pH 7.8 + 20 mM KCl + 0.02% Tween 20 + 1 mM TCEP + 10 mM Na ₂ SO ₃ 15 minutes at room temperature
Running buffer	1x TAE 0.5x TBE
Protein concentration (pmol)	0; 100; 200; 300; 400; 500; 1000

The reaction mixtures were applied to a 2% agarose gel, which had been running for 1 h at 80 V in running buffer 1x TAE (Tris base, acetic acid and EDTA) 0.5x TBE (Tris, boric acid and EDTA). The compound TCEP is an additive present in some incubations and it is used as a reductant. The DNA was visualized with SYBR Green dye.

Thermofluor assay

Thermofluor assay is a technique that monitors the loss of secondary structure with a temperature increase, through a fluorescent probe, SYPRO® orange (Thermofisher), which binds to the hydrophobic parts of the protein, revealing the protein denaturation.

The thermal shift assay was performed on an iCycle iQ5 Real Time PCR Detection System (Bio-Rad), varying:

- a) Protein concentration and the dye dilution factor, variables that influence the signal strength;
- b) Sulfur ligands.

The amount of protein tested were 10 µg, 26 µg and 52 µg and the dye concentration tested was 5 fold, 10 fold and 20 fold (diluted from the initial 5.000-fold stock in 50 mM HEPES pH 8.0). The protein was subjected to thermal denaturation, heated from 20 °C to 90 °C in a stepwise gradient (one degree per minute), and the dye allows a fluorescence reading. The best conditions of signal/noise ratio obtained were using 26 µg protein and 20-fold dye. These were the conditions used in the remaining assays. The sulfur ligands tested were sodium sulfite and sodium sulfide in different ratios, from 1/0.5 to 1/20 (protein/ligand), aiming to see a protein stabilization that indicates that the protein interacts with the sulfur ligands.

DsrD Expression Differences

To obtain insights into the physiological role of the DsrD protein, *Desulfovibrio vulgaris* Hildenborough was grown in anaerobic conditions in a rich medium with 20 mM Lactate as electron donor, 20 mM of different electron acceptors (sulfate, thiosulfate or sulfite) and geneticin (100µg/mL), at 37 °C, during 30 hours. The cells were harvested by centrifugation at mid-exponential and end of exponential, resuspended in 50 mM potassium phosphate pH 7.4, 10% glycerol with protease inhibitor cocktail and lysed in a Minilys. The expression of DsrD protein in different conditions was analyzed through Western Blot, as described above.

Far Western Blot

We used 10 µg of pure DsrAB, DsrC and DsrMKJOP proteins from *Desulfovibrio*, previously purified in the laboratory, that were subjected to a 10% Tricine-SDS-PAGE and then blotted to a 0.22 µm PFDV membrane (Roche). The membranes were dried overnight and then incubated with DsrD (25 nM) for 1 hour in TBST and 1.2% dry milk. The membrane was washed with TBS. Western Blot was performed using primary antibody anti-rabbit Anti-His tag (1:30.000) for 1 hour in TBST, followed by 45 minutes incubation with the secondary antibody, anti-Mouse IgG conjugated with alkaline phosphatase (1:7.500, Sigma). The protein detection was performed as described above. As negative control the same proteins were not incubated with DsrD, and as positive control DsrD was used.

Purification of *Bilophila wadsworthia* DsrABC

Bilophila wadsworthia (DSM 11045, strain RZATAU) was previously grown in DMZ 503 medium with formate and taurine, and bubbled with N₂ + CO₂. The collected cells were resuspended in 25 mM potassium phosphate pH 7 in the presence of DNase and broken in a French Press (figure II.1A). The cell extracts were centrifuged at 10.000 g for 15 minutes to remove cell debris and the supernatant was then ultracentrifuged at 144.000 g for about 2 hours to remove the membrane fraction. The soluble fraction was loaded into a Q-Sepharose high performance column (figure II.1B) equilibrated with 25 mM potassium phosphate pH 7.0. The proteins were eluted with different concentrations of potassium chloride and the presence of DsrABC protein in each fraction was analyzed by the ratio of the absorbance at 280 nm and the characteristic peak at 630 nm for DsrAB. The protein was eluted with 300 mM of potassium chloride.

The fractions were subjected to a 10% Tricine-SDS-PAGE gel and to a 9% native gel. The analysis of these gel suggested two forms of DsrABC, with different pIs and/or molecular weights, indicating that the samples were not homogenous. Therefore, the proteins were separated in a 9% Acrylamide gel containing 0.1% triton X-100 under native conditions (figure II.1C), as described to purify DsrABC from *DvH* [37]. Given the green color of the protein it was possible to identify two different bands in the gel without any staining. These bands were cut in small pieces and submitted to an electro-elution on a Bio-Rad electro-eluter (model 422) (12 mA, 3 h + 9 mA, 2 h, 4 °C) in transfer buffer (figure II.1D). After electro elution the samples were collected, washed in 50 mM potassium phosphate pH 7.0, concentrated, and then used for crystallization and kinetic studies.

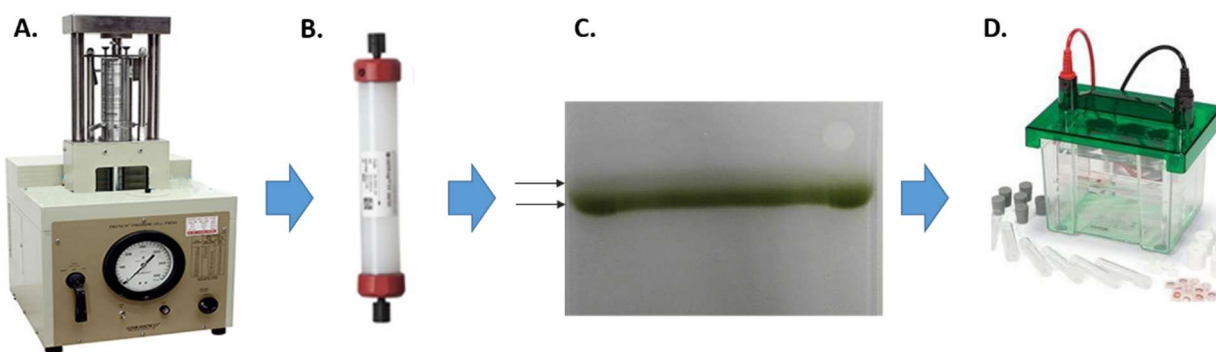


Figure II.1 – Purification of DsrABC from *Bilophila wadsworthia*

Kinetic Studies

The kinetic parameters for sulfite reduction by DsrABC of *Bilophila wadsworthia* were not determined yet. The enzymatic reduction of sulfite was executed in an anaerobic chamber (95% Ar, 5% H₂) at 37 C using reduced methyl viologen as electron donor. The methyl viologen was previously reduced with zinc granulates, and sodium sulfite was used as electron acceptor and as reaction starter.

For the determination of the protein concentration that allows a steady state, the protein concentration was varied. The assay was carried out in 50 mM potassium phosphate pH 7, adding 1 mM reduced methyl viologen, 0 to 500 nM of DsrABC and 500 μM of sodium sulfite. For the determination of kinetic parameters, the assay was performed in 50 mM potassium phosphate pH 7, adding 1 mM reduced methyl viologen, 140 nM of DsrABC and 0 to 1 mM sodium sulfite. These assays were repeated with 25 nM of protein. The methyl viologen oxidation was monitored at 732 nm ($\epsilon = 3.15 \text{ mM}^{-1} \text{ cm}^{-1}$) in a spectrophotometer (Shimadzu UV-1800).

Purification of DsrAB from IPFG07 strain

To study the mechanism of the DsrC trisulfide production in *Desulfovibrio vulgaris* we used the IPFG07 strain, described in [35]. In this strain the chromosomal *dsrC* was deleted from the genome and a plasmid containing the wild-type *dsrC* with a relatively weaker promoter was inserted. This plasmid also allowed the insertion of a His-Tag in the DsrC protein that will be expressed in lower amounts than DsrAB.

The IPFG07 strain was grown in a lactate-sulfate medium, then the cells were collected by centrifugation and resuspended in the 50 mM potassium phosphate pH 7.0 (buffer A) with protease inhibitor cocktail and DNase, and broken in a French Press. The cell extracts were centrifuged at 10.000 g for 15 minutes to remove cell debris and the supernatant was then ultra-centrifuged at 144.000 g for about 2 hours to remove the membrane proteins. The soluble fraction was loaded into a Q-Sepharose 26/10 high performance column equilibrated with buffer A, and elution was made in a stepwise increase of NaCl concentrations. The fractions were analyzed in 10% Tricine-SDS-PAGE, native gel, and DsrAB characteristic peak at 630 nm. Those that show presence of DsrAB were the fractions eluted between 300 and 400 mM of Sodium Chloride. The fractions containing DsrAB (peak 630 nm) were loaded in a HiTrap IMAC column charged with nickel and equilibrated with 50 mM potassium phosphate and 400 mM NaCl. The protein was eluted with a stepwise increase of imidazole. The samples were collected, washed in 50 mM potassium phosphate pH 7.0, concentrated, subjected to 10% Tricine-SDS-PAGE, and transferred to 0.22 μm PDVF membrane (Roche) at 100 V in a Mini Trans-Blot wet cell (Bio-Rad) for 8 minutes. The membrane was dried overnight and incubated with primary antibody Anti-DsrC (DsrC antiserum, 1:10.000) for 1 hour in TBST containing 1.2% dry milk, followed by incubation with the secondary antibody, anti-rabbit IgG conjugated with alkaline phosphatase (1:15.000, Sigma). The protein detection was performed with Alkaline Phosphatase Buffer and NBT/BCIP solutions.

Purification of DsrC

A recombinant plasmid containing the *dsrc* gene with a mutation in a non-catalytic cysteine, changed to an alanine (*drsC Δ C_26_A* DvH) in pET-28a-c(+) vector (Novagen®), which allows insertion of a 6x-His tag at the C-terminus, was transformed in *E. coli* BL21-Gold(DE3) that were grown at 37 °C in M9 minimal medium with ampicillin (100 $\mu\text{g}/\text{mL}$) until optical density of 0.5. Then 100 μM IPTG was added and cells were grown for 5 additional hours.

The cells were harvested by centrifugation and resuspended in 25 mM potassium phosphate, 300 mM NaCl and 30 mM imidazole pH 7.0 (buffer A), disrupted through mechanical lysis with glass beads in a Minilys (Bertin technologies), then centrifuged at 13300 rpm for 20 minutes. The supernatant was loaded into the HiTrap column charged with nickel and equilibrated with buffer A, and eluted with the same buffer plus 150 mM imidazole. The protein was dialyzed to 50 mM potassium phosphate pH 7.0, the purity was analyzed by 10% Tricine-SDS-PAGE and the concentration was determined at 280 nm using an absorption coefficient of 18.6 $\text{mM}^{-1}\text{cm}^{-1}$.

Kinetic assays

In *Archaeoglobus fulgidus* it was described that the DsrC protein forms a trisulfide [35]. Here the assay was conducted as described, inside the anaerobic chamber with 50 mM potassium phosphate pH 7.0, 1 mM reduced methyl viologen, 430 nM of DsrAB, sodium sulfite and recombinant DsrC (7.5 μ M and 30 μ M). The DsrC protein used in the study was previously reduced with 5 mM dithiothreitol (DTT) during 30 minutes at 37 °C, and the excess of reductant was removed with a HiTrap Desalting column (GE Healthcare). The redox state of the cysteines was monitored with the MalPEG (methoxy-polyethylene glycol maleimide) gel-shift assay, that binds to free cysteines and causes an increase in the molecular weight of the protein by 10 kDa per each reduced cysteine [39]. From the assay mixture, about 5 μ g of DsrC was incubated with 1 mM MalPEG for 15 minutes at 37 °C inside the anaerobic chamber. After the reaction the sample was analyzed by 10% Tricine-SDS-PAGE under non-reducing conditions. The reduced DsrC was also subjected to the same treatment as control for MalPEG binding.

III. Results and discussion

Characterization of DsrD

Purification of DsrD

For the characterization of DsrD, the protein was purified as described from *E. coli* cells. The purification gave rise to two fractions, one that was eluted with 100 mM of imidazole and another with 500 mM of imidazole. Both fractions were analyzed and subjected to a 10% Tricine-SDS-PAGE (figure III.1A), to check the purity; and one of the samples was treated in non-reducing conditions to see if there was formation of dimers.

The concentration of the first fraction was determined from the absorbance at 280nm (figure III.2B) and $\epsilon=9.9 \text{ mM}^{-1} \text{ cm}^{-1}$. The first fraction was used in the subsequent studies, with the final concentration of 13.1 mg/mL.

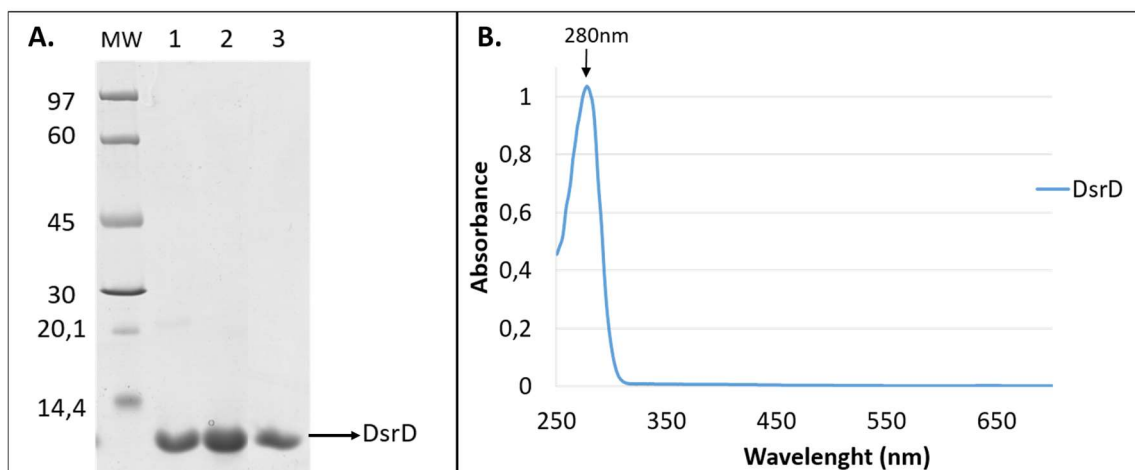


Figure III.1 - Purification of DsrD. A) Tricine-SDS-PAGE; MW- molecular mass markers (kDa); 1- First fraction eluted at 100 mM of imidazole; 2- Second fraction eluted at 500 mM of imidazole; 3- First fraction in non-reductive conditions (5 μg of protein). B) UV-Vis spectrum of DsrD.

The DsrD protein has a molecular weight 8.8 kDa and since the purified protein has a His-Tag insertion its final molecular weight is around 9.8 kDa, so the band in the gel is lower than 14.4 kDa, as expected. Since there are no more bands present in the gel, the purification of DsrD was successful, and there was no evidence of dimer formation. The UV-Vis spectrum also does not show any characteristic peak other than the expected peak at 280 nm.

Western blot

The Western blot technique was used to analyze the differences in expression of DsrD under different growth conditions in order to try to get a relationship between expression and function of DsrD, which is unknown. For this analysis, it was necessary to optimize the protocol in order to obtain a good and measurable signal for DsrD protein, using the anti-DsrD antibody already available in the laboratory.

This optimization process for Western blotting was done in steps evaluating several parameters. First the dilution of the first anti-DsrD antibody, then the transfer time to the PDVF membrane and the total amount of the protein extracts that allows having a quantitative signal for DsrD. In the first assays, we could observe that DsrD is not very stable in the protein extracts, so multiple cell growths were headed for all the tests. Due to this instability, it was also tested if a different lysis process allowed a lower protein degradation, namely mechanical lysis and bug buster lysis. Bugbuster is a commercial kit that uses a mixture of detergents for the disruption of the *E. coli* cell wall allowing the extraction of the soluble proteins.

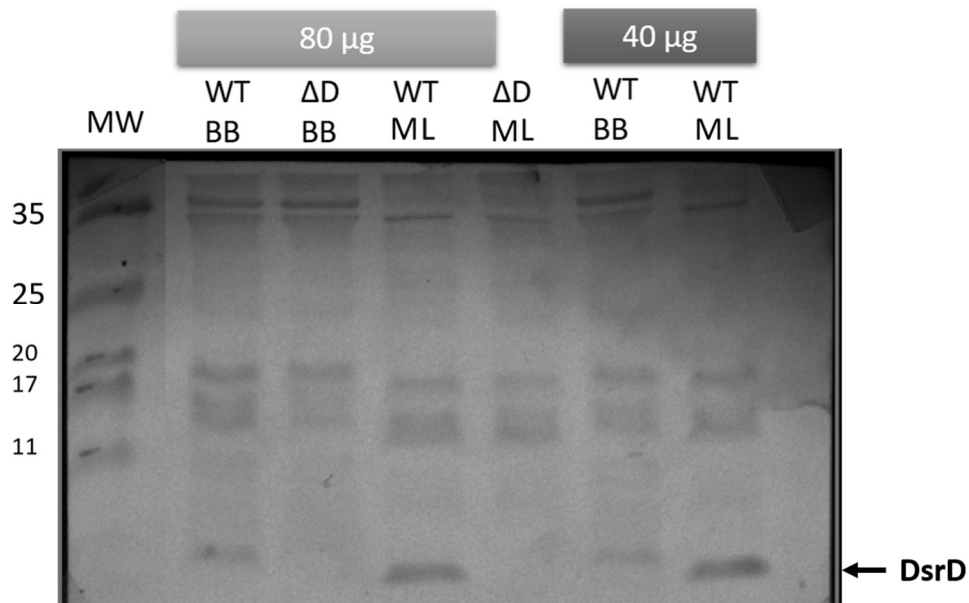


Figure III.2 - Western blot optimization results. MW - Molecular weight (kDa); WT - wild type *DvH*; ΔD - *DvH* mutant without *dsrD* gene; BB - lysed with Bug Buster; LM - lysed by mechanical lysis, with MiniLys; 40 and 80 μg of total protein extract were used.

The optimal conditions obtained for the Western blot were: seven minutes of transfer to PVDF membrane in the Mini Trans-Blot wet cell (Bio-Rad), 1:5000 dilution of anti-DsrD primary antibody and the optimal amount of total protein extract was 80 μ g (figure III.2). The best lysis mechanism proved to be the mechanical lysis, where the protein did not have so much degradation, allowing a better signal, probably because some component of Bug Buster caused protein degradation. The subsequent studies were all made using protein obtained with these conditions. In all Western blots done during the optimization process, the mutant strain, where the *dsrD* gene was deleted from the genome, was also ran as a negative control for nonspecific signals. Since there were no unspecific signals in the 10 kDa zone, the subsequent studies were made just with the wild-type *DvH* grown in different conditions.

Growth studies

With the objective of understanding the function of DsrD, an analysis of its expression in *DvH* was made using different electron acceptors, such as sulfate, sulfite and thiosulfate, and at different points during the growth curve (mid-point exponential and late exponential/beginning of stationary). This analysis may give some light about the conditions and moment of the growth curve this protein has more relevance. The expression analysis was made using the Western-blot technique.

The *DvH* growths were conducted in a rich medium (supplementary data), supplemented with 20 mM lactate, as electron donor, and 20 mM of the different electron acceptors, as described above. The bacteria showed the ability to grow with all the electron acceptors, as expected, but did not achieve the same optical density. With sulfate and sulfite, the maximal optical density was around 0.6 and with thiosulfate it was around 0.45 (figure III.3), showing that the bacteria were more efficiently growing in sulfate and sulfite.

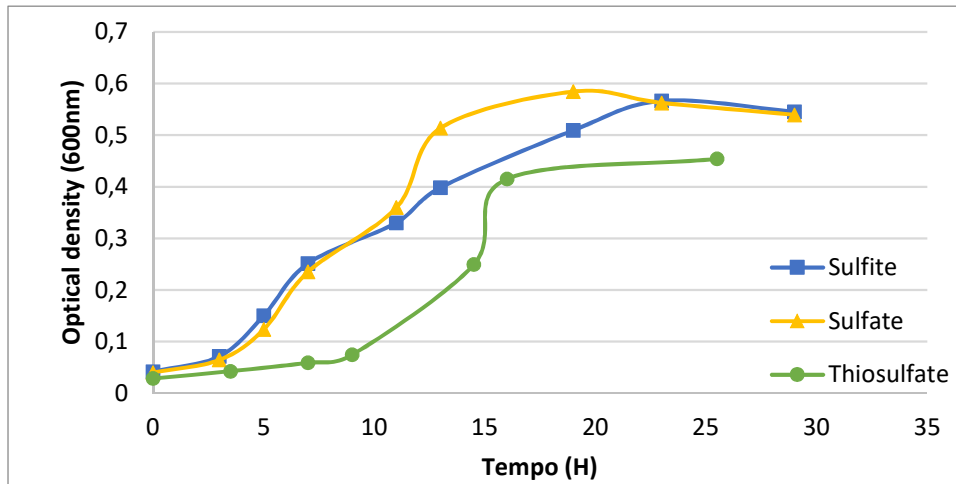


Figure III.3 - Growth curves of DvH with different electron acceptors: Sulfate, sulfite, and thiosulfate.

Samples of the DvH cells were taken at mid-point and at the end of the exponential growth curves. The samples were treated as previously described and analyzed by Western blot using anti-DsrD to check if there were any significant expression differences that could help explain the function of DsrD in sulfate reduction.

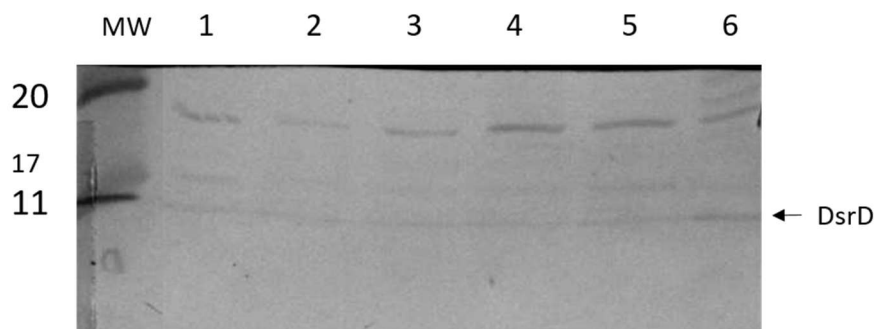


Figure III.4 – DsrD expression in different growth conditions. MW – Molecular weight marker; 1, 2, 3 - samples taken at mid-point exponential phase from sulfate, sulfite, and thiosulfate grown DvH cells, respectively; 4, 5, 6 - samples taken at the end of exponential phase from sulfate, sulfite, and thiosulfate grown DvH cells, respectively.

The results are shown in figure III.4, and there were no considerable differences in the different electron acceptors or in the stage of the growth curve, so no insight into the function of DsrD could be obtained.

Possible role in regulation

The crystal structure of DsrD suggests that it has a DNA binding motif. To analyze if the protein has a regulatory role on the *dsr* operon, the *dsr* promoter region was amplified from the genomic DNA of DvH using PCR, then was subjected to an agarose gel and purified with the Agarose extraction kit. The resulting fragment has around 500 base pairs (bp). The DsrC protein was also tested since in *Allochromatium vinosum* this protein was shown to bind to the *dsr* promoter region [46], and we wanted to analyze if it has the same effect under the same conditions in DvH.

The amplified DNA was incubated with DsrD and DsrC proteins, separately, in the conditions described in methods. If the DNA interacts with the proteins, it would be retarded in the gel relative to the non-protein bound DNA (figure III.5B).

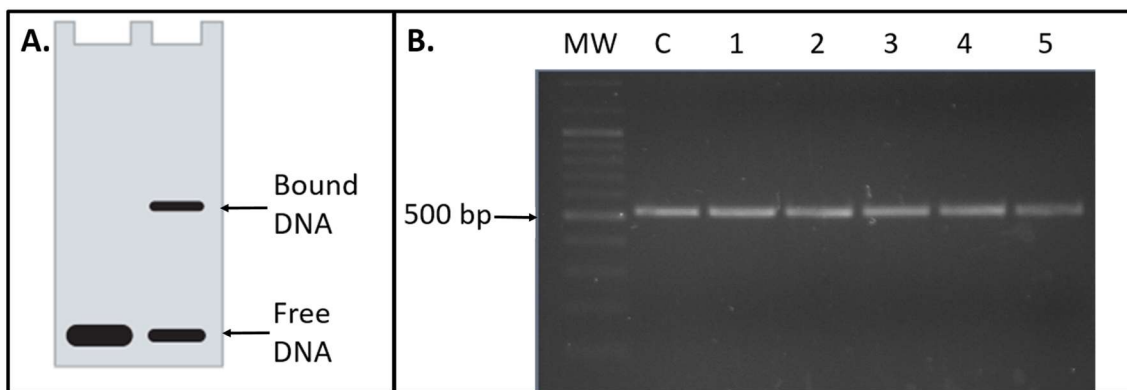


Figure III.5 - Electrophoretic mobility shift assay. A) schematic representation of the assay, with free and bound DNA; B) example of the results obtained, MW - DNA markers, C - DNA with no protein; 1-5 DNA incubated with increasing concentration of protein from 100 to 500 pmol of protein.

In all the conditions tested we never observed a DNA shift. The protein concentrations tested were from 100 to 500 pmol of protein with 200 fmol of DNA. The negative results show that at least in the tested conditions [45, 47], the DsrC and DsrD proteins do not interact with the *dsr* promoter region (figure III.5), so we could not find any indication that either DsrD or DsrC act as regulatory proteins using the described method.

Thermofluor assays

Thermofluor assays measure protein stability in different conditions by monitoring protein denaturation as a function of temperature using a fluorophore called SYPRO orange dye.

The protein is incubated with different additives and compared with the original control condition to understand if there is stabilization (the melting temperature T_m increases, so the protein denatures at higher temperatures), destabilization (decreasing of the T_m), or no change. The protein is incubated with the dye and the additives, to study its interaction.

In this study, we aimed to evaluate the interaction between DsrD and sulfite (sodium sulfite, Na_2SO_3) and sulfide (Sodium sulfide, Na_2S), by incubating the protein with different protein to ligand ratios. The amount of protein and ratio to the dye needed to see the reaction was initially tested and the best condition found was 26 μg of protein and 20 fold excess of the dye relative to the protein in the reaction mix. The results are shown in table III.2.

Usually this technique is used with proteins with higher molecular weights, and in those cases the protein amount needed is lower, as well as the dye concentration. Since DsrD is a very small protein with only 9.8 kDa, the amounts of protein and dye needed to observe fluorescence was very high.

Table III.2 – Melting temperatures in the different conditions tested. The results shown are the average of triplicates.

Ratio (protein to sulfur)	T_m ($^{\circ}\text{C}$)	
	Na_2SO_3	Na_2S
1:0,5	64,0 \pm 0	63,7 \pm 0,9
1:1	63,0 \pm 0	64,0 \pm 0
1:2	64,0 \pm 0	62,7 \pm 0,4
1:5	63,7 \pm 0,4	64,0 \pm 0
1:10	63,4 \pm 0,4	—
1:20	63,4 \pm 0,4	64,7 \pm 0,4
Protein only	64,5 \pm 0,5	

The results show that there is no considerable alteration of the protein stability in the presence of the sulfur compounds tested, indicating that maybe it does not interact with either of these compounds since the melting temperature is not significantly altered comparing to the protein alone.

Far-Western blot

Since there was no evidence that DsrD interacted with DNA or sulfur derivatives, we investigated if DsrD interacts with other proteins that are involved in the sulfite reduction electron transfer pathway. The technique used to study a possible interaction was the Far Western blot. In this technique, the possible interacting proteins are subjected to a Tricine SDS-PAGE gel and transferred to a PVDF membrane. The membrane is incubated with the protein of interest, in this case DsrD, washed and then the Western Blot analysis against DsrD is performed. In our study the proteins tested were DsrABC, DsrMKJOP (membrane complex) and DsrC, which once transferred to the membrane were incubated with DsrD, followed by Western blot analysis. A control experiment was done where the membrane was not incubated with the protein and the anti-DsrD Western blot was performed to see if there were any unspecific signals. The assay was done in triplicate and the results were similar in all.

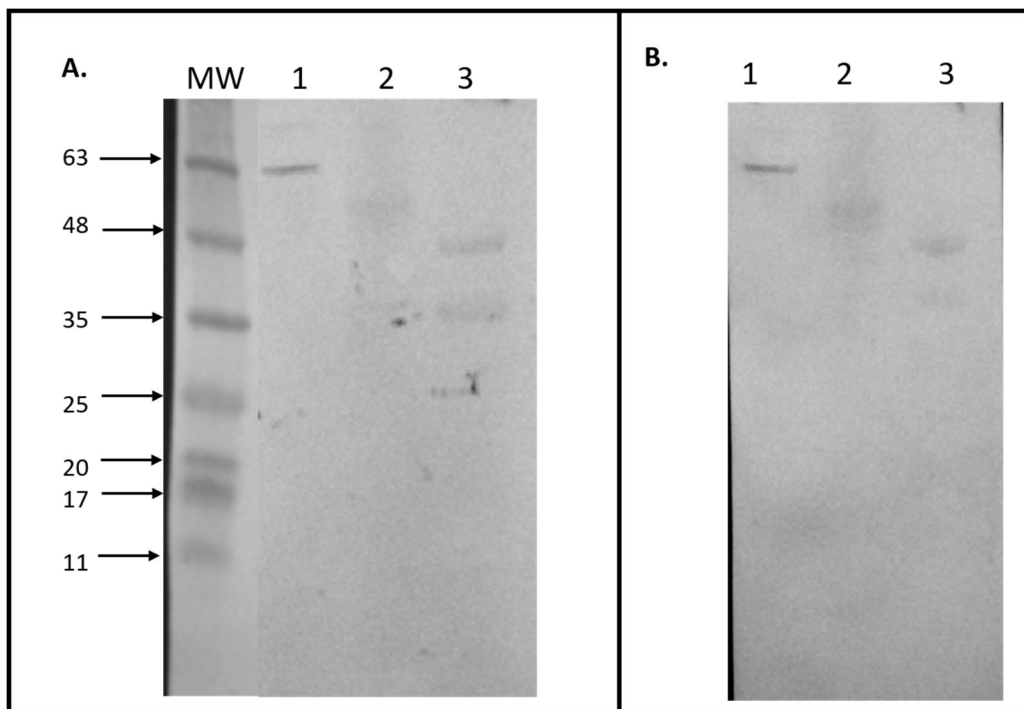


Figure III.6 - Far Western Blot Results. A) membrane incubated with DsrD protein; B) Control membrane, without incubation; 1 – DsrAB, 2 - DsrMKJOP, 3 – DsrC, 4 - DsrD.

The pattern observed in the assay (membrane incubated with DsrD) and in the control experiment (with no incubation with DsrD) is very similar (figure III.6). Both membranes have the same spots, indicating that the all the signals are non-specific, indicating that DsrD does not

interact with any of the proteins tested in the conditions of the study. The fact that there is no binding in the assay does not mean that *in vivo* the proteins do not interact in some way, since the interaction might need special conditions or chaperones. The DsrAB is pointed as one of the proteins that can interact with DsrD, since these proteins are found in the same operon and DsrAB has a crucial role in the sulfite reduction.

Bilophila wadsworthia**Protein purification**

In the genome of *B. wadsworthia*, unlike in sulfate reducing organisms, the DsrD is fused with DsrB, indicating the involvement of the DsrD protein in sulfite reduction. The determination of the crystal structure of this protein might unveil the DsrD function, since we will be able to see how DsrD interacts with DsrAB. The protein was also used to measure the specific activity in order to kinetically characterize it and to study the impact of having a fusion protein (DsrB + DsrD) in the process by comparing the kinetic differences of other DsrAB that do not have a fused DsrD.

Purification of DsrABDC from *B. wadsworthia* was performed according to the reported protocol for DsrABC from *DvH* [37], which was the purification method that allowed us to obtain the protein crystal structure of the *DvH* protein, since it had multiple oligomeric forms and it was the only way to separate them. The purification started with an ion exchange chromatographic column, eluted with increasing concentrations of salt ions. The protein was eluted with 300 mM of KCl (chromatogram in supplementary data) and analyzed through SDS-PAGE gels and UV-vis spectra, looking for the characteristic peak at 630 nm. The chosen fraction was concentrated and subjected to separation using a native gel. The protein band was seen by naked eye since it is a green colored protein. It was possible to see two bands close together, and the bands were divided into fragments that were electroeluted. The resulting fractions were concentrated and washed with the same buffer that was used for the kinetic studies (50 mM potassium phosphate pH 7). The concentration was determined by absorbance at the 630 nm peak with $\epsilon_{630} = 53 \text{ mM}^{-1} \text{ cm}^{-1}$. The purification process was repeated twice, at different times. The concentration results are in table III.3. The purified protein was also analyzed by gel and compared with DsrAB from *DvH* (figure III.7).

Table III.3 – Concentrations obtained in both batches of the purification in the two main fractions containing DsrABDC.

1 st Batch	2 nd Batch
#1.1 = 13.7 mg/mL	#2.1 = 10.3 mg/mL
#1.2 = 11.6 mg/mL	#2.2 = 9.8 mg/mL

C

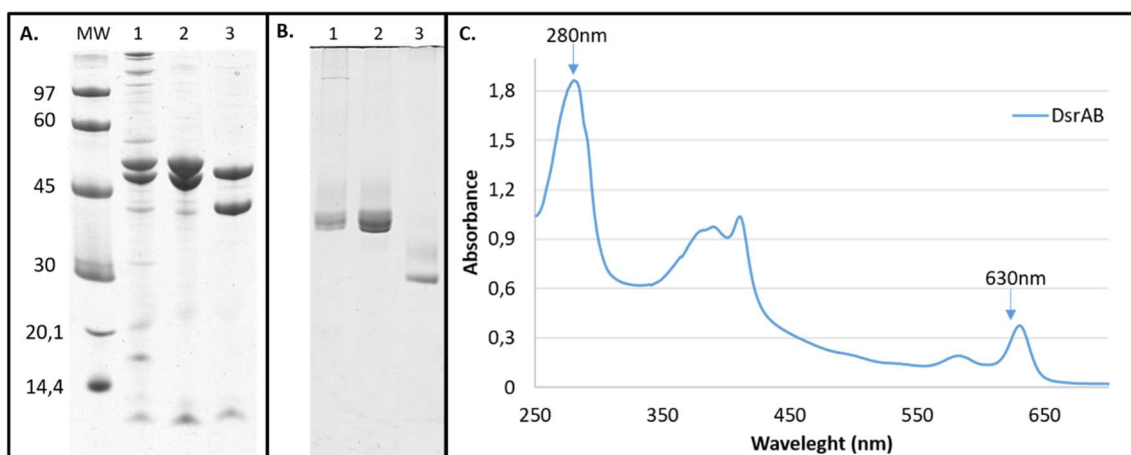


Figure III.7 - Purification summary. A) Tricine-SDS PAGE gel. B) Native gel; in A and B panels lane 1- fraction after the chromatographic step; lane 2 - fraction 1.1 after the electro elution purification step; lane 3 - DvH DsrABC. C) UV-vis spectrum of purified DsrABDC from *B. wadsworthia*

The purification method proved to be successful also for DsrABDC from *B. wadsworthia* and, as expected, the DsrA subunit is almost of the same molecular weight as the DvH DsrA (around 50 kDa), and the DsrB subunit from *B. wadsworthia* has a higher molecular weight than the DvH DsrB (around 40 kDa), since it is a fusion protein with DsrD (total 54 kDa). DsrC was also found to co-purify with DsrABCD from *B. wadsworthia*, as in the case in DvH (band at 12 kDa) [37].

Kinetic Characterization

In the sulfite reduction assay the methyl viologen is previously reduced, and it is used as an electron donor to that enzyme so the DsrABDC is able to reduce sulfite. The MV oxidation can be followed by a decrease in the absorbance at 732 nm in a spectrophotometer, and the regression coefficients can be measured and converted to activity (mU/mL).

The fraction 1.1 was used for kinetic assays. The first study was used to discover at which protein concentration the activity is proportional to the protein concentration (Figure III.8). For this, the concentration of substrate used was always the same and in large excess, and the amount of protein was gradually decreased. One of the difficulties in the study of this protein was its degradation and the loss of activity after some time, even if the protein was kept at 4 °C in anaerobic conditions, leading to the need for a second purification, and the repetition of the kinetic profiles.

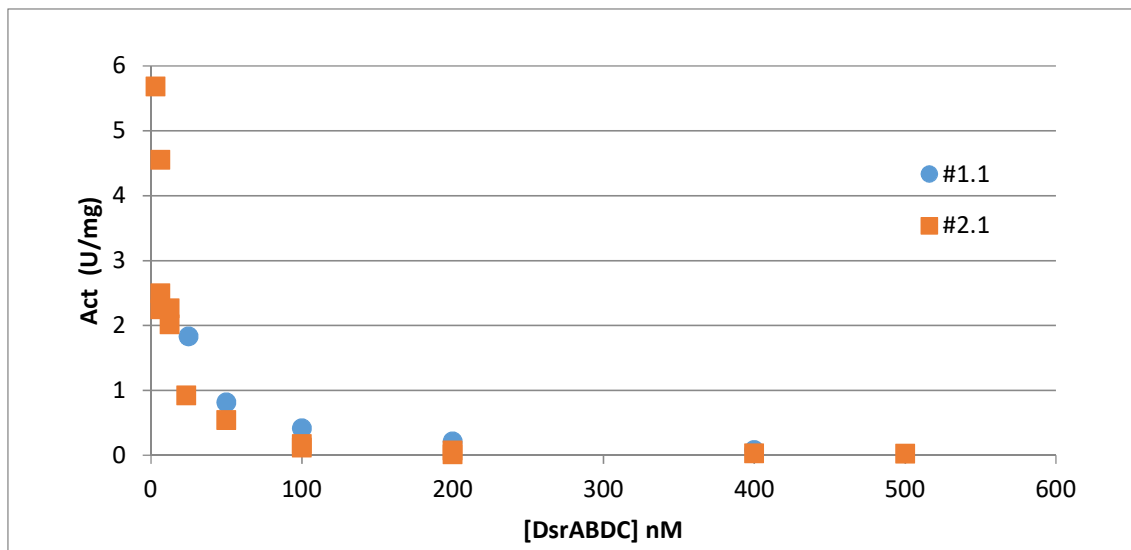


Figure III.8 – Activity versus concentration of protein. Assays performed at 35 °C with sulfite concentration of 500 μ M. In blue dots are the results for the first batch #1.1 and in orange squares the results for the second batch #2.1.

This study is necessary to determine the protein concentration to be used for the determination of the kinetic curve. For the reasons mentioned above the assays were done with the two batches, with the fractions #1.1 and #2.1. For the following study the fraction #1.1 was used with 140 nM of protein and for the fraction #2.1 we used 25 nM of protein.

After fixing a protein concentration the kinetic curve was determined by measuring activity versus sulfite concentration (Figure III.9). This study was made maintaining the concentration of the enzyme previously determined, allowing to see the enzyme rate response to the alteration of substrate concentration. With the increase in substrate concentration, the activity increases, and the resulting curve indicates that the enzyme follows Michaelis–Menten kinetics.

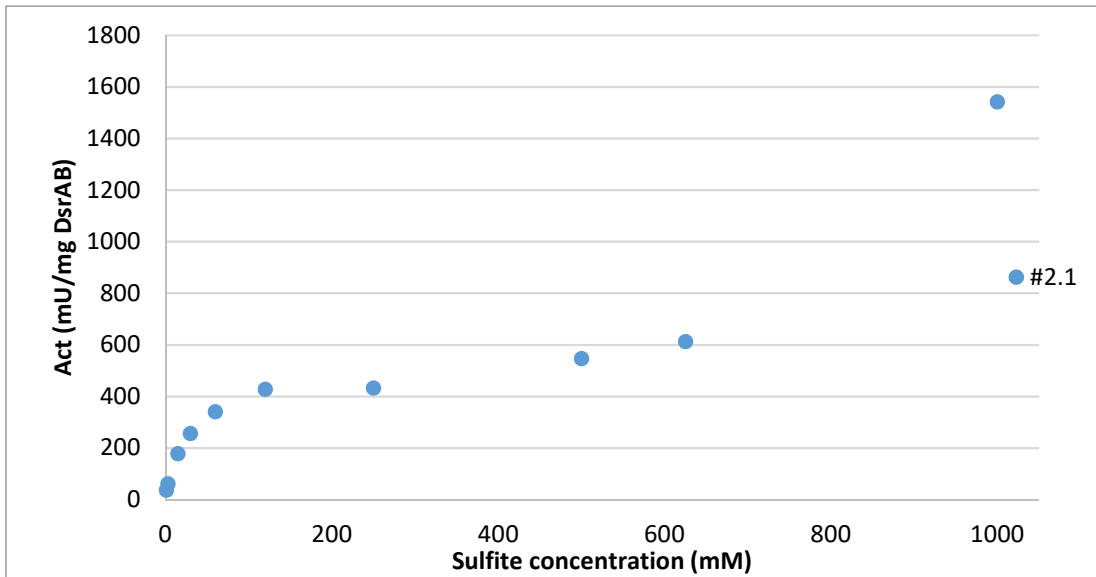
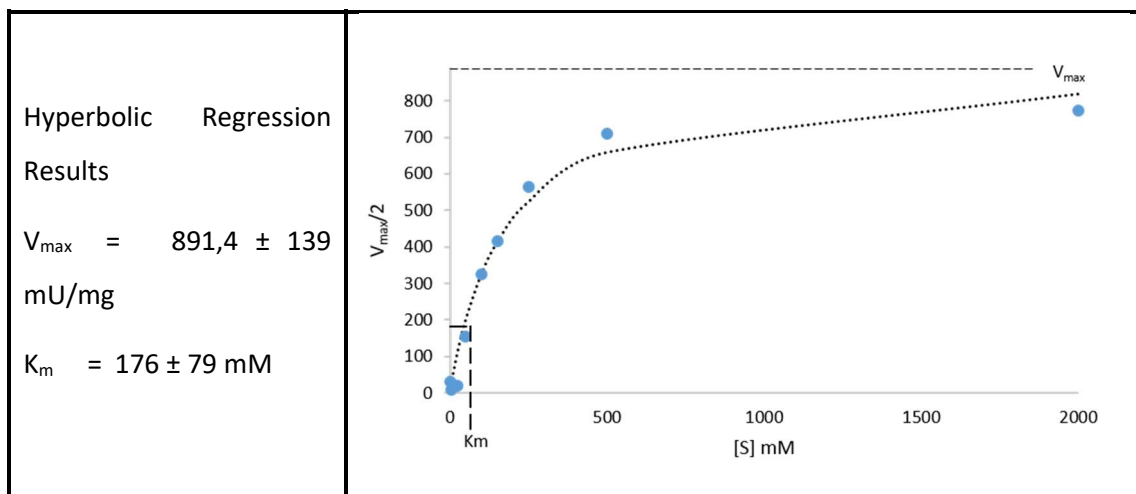


Figure III.9 - Activity versus sulfite concentration at 35 °C. In blue dots are the results for #2.1 with the protein concentration of 25 nM.

The Hyper 32 program was used to fit the results and determine the kinetic parameters through the hyperbolic regression method. V_{max} represents the maximum reaction rate achieved, and K_m is the substrate concentration needed to achieve half of V_{max} , in Michaelis-Menten kinetics. This process was done with the two fractions that gave rise to different results. Since the kinetic curve was more defined in the first purification batch, the results corresponding are shown in table III.4.

Table III.4 – Hyper 32 fitting results for Hyperbolic Regression, and the hyperbola graph obtained.



In order to try to evaluate the effect of DsrD in the DsrABDC enzyme from *B. wadsworthia* we can compare its kinetic parameters obtained in this work with those of DsrABC from DvH and with DsrAB+DsrC from *A.fulgidus*, as in these cases DsrD is absent (table III.5). In terms of V_{max} , the DsrABDC from *B. wadsworthia* has a higher sulfite-reduction rate (3.7-fold higher) than DsrABC from DvH, which is the example that allows a better comparison as in both cases DsrC co-purifies with DsrAB.

Table III.5 – Summary table for the kinetic parameters for Dissimilatory sulfite reductases from different organisms

<i>Bilophila wadsworthia</i> DsrABDC	DvH DsrABC [48]	<i>Archaeoglobus fulgidus</i> DsrAB+DsrC [35]
$V_{max} = 891,4 \text{ mU/mg}$ $K_m = 176 \pm 79 \text{ mM}$	$V_{max} = 238 \text{ mU/mg}$ $K_m = 4,1 \text{ mM}$	$V_{max} = 1278 \pm 2 \text{ mU/mg}$ $K_m = 12 \pm 3 \mu\text{M}$

The differences observed in table 5 in enzyme kinetics of *B. wadsworthia* versus other organisms, can be due to DsrB being a fusion protein with DsrD. This protein is positively charged and this fusion can influence the folding of the DsrB catalytic subunit or the substrate channel, making the enzyme have less affinity for substrate binding, which may explain the high K_m of the enzyme. In contrast, the maximal velocity is higher for *B. wadsworthia* than for DvH.

Crystallographic studies

One of the goals of the project was to solve the crystal structure of DsrABDC from *B. wadsworthia*, to try to understand the role of DsrD at the structural level, so the protein was sent to the Membrane Protein Crystallography Lab at ITQB where crystallographic screenings were performed, resulting in some green colored protein crystals (Figure III.10).



Figure III.10 - Crystal of DsrABDC protein, from the screening of crystallographic conditions.

The optimization of these crystals to a bigger scale and non-needle crystals is being carried out by the collaborators with protein from both purifications.

DsrAB from IPFG07 and DsrC_C26A

Archaeoglobus fulgidus is an organism where it is reported that DsrAB can be isolated separately from DsrC and where kinetic studies showed a significant increase in DsrAB activity when DsrC is added to the reaction [35]. Our aim was to study this interaction in DvH proteins, where DsrAB can not be isolated separately in the wild type, so there was a need to use a mutant strain. In the IPFG07 strain the *dsrC* gene is deleted from the genome and a plasmid with the *dsrC* gene was inserted. The need to insert DsrC in a plasmid is because the organism is inviable without this crucial protein. The plasmid also allowed the insertion of a His-Tag in DsrC, that will allow the protein to be separated from DsrAB with an affinity column. This method allows a lower expression of DsrC compared to the wild type and simultaneously increases the probability of having DsrAB free of DsrC. With this strategy we aim to reproduce the DsrC trisulfide product described in *A. fulgidus* using the DvH proteins.

Protein purification

The purification of DsrAB without DsrC was performed from the IPFG07 strain, which has the *dsrC* gene deleted from the genome and expressed in smaller amounts from a plasmid. First, the soluble fraction of IPFG07 was subjected to an ion exchange column to separate DsrAB from the other proteins of DvH. The fractions that contained DsrAB were then loaded in a nickel column, taking advantage that the DsrC expressed from the plasmid has an N-terminal His tag, which allowed us to retain DsrC in the column and elute the DsrAB enzyme. The protein in complex with DsrC was then eluted with increasing concentrations of imidazole.

DsrABC was eluted from the first Q-sepharose column, from 300 to 400 mM of NaCl and divided into four fractions, corresponding to the four peaks (chromatogram in Supplementary data). From earlier studies – performed in the laboratory – it was expected that the first peak eluted from the ion exchange column containing DsrAB would be the fraction where there was more protein in complex with DsrC, so the other three peaks were loaded separately in the nickel affinity column and eluted with imidazole. In all the elutions from the second purification step (figure III.11A), the first two fractions were the ones that had DsrAB without DsrC bound. The protein purity was analyzed by Tricine-SDS-PAGE gel and the presence of DsrC in the multiple eluted fractions obtained from the nickel column was analyzed by Western blot.

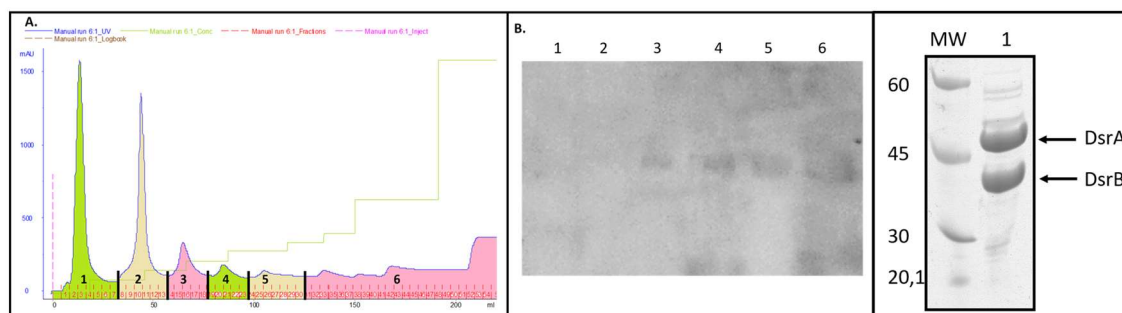


Figure III.11 - Purification of DsrAB from the IPFG07 mutant. A) Chromatogram of HiTrap IMAC affinity column. 1 to 6 represents the fractions obtained from the elution with increasing steps of imidazole. B) Western blot against DsrC with the fractions from the chromatogram (30 μ g of protein). C) SDS-Page of DsrAB, 1 – DsrAB from IPFG07.

The purification of DsrAB lacking DsrC from the IPFG07 strain was possible, as the Western blot analysis shows that in some of the fractions there was no DsrC present. The DsrAB-DsrC complex was only eluted in the fractions with increasing amounts of imidazole (figure III.11B). The DsrAB-DsrC started being eluted with 50 mM of imidazole (fraction 3), and the fractions used for the subsequent studies were the 1st and 2nd fractions, that did not show any DsrC protein.

In the *DvH* DsrC_C26A, a DsrC variant where the cysteine that is not involved in the catalytic activity, Cys26, was replaced by an alanine, the only cysteines present are the catalytic ones. This DsrC variant was cloned in pET28a plasmid with a His-Tag at the N-terminus, and transformed in *E. coli* BL21 (DE3) Gold. The protein was expressed and purified from *E. coli* using a HiTrap column, eluted with 150 mM of Imidazole, and then washed and concentrated. For the kinetic assays, the protein was always previously treated with DTT so that the cysteines were reduced and available to work with DsrAB in sulfite reduction. The excess of DTT was removed using a BioSpin column.

Kinetic Assay

The aim of this study was to see if there is an increase in DsrAB enzymatic activity when DsrC is added to the reaction, as observed for *A. fulgidus* DsrAB/DsrC [35]. The DsrAB was added to reduced methyl viologen in a concentration of 150 nM, and then sulfite was added at a concentration of 500 μ M. The DsrC was added at 7.5 μ M and 30 μ M, and in the control experiment, no DsrC was added, mimicking the assay conditions recently published (figure III.12). If the enzyme activity increases due to the addition of DsrC we should observe a stronger

decrease in the absorption at 732 nm due to the oxidation of the methyl viologen. In vivo, the role of DsrAB is to reduce sulfite, and in *A. fulgidus* the DsrC was shown to bind the sulfur atom of sulfite between its cysteines producing a trisulfide state, leading to a two-phase reaction plot.

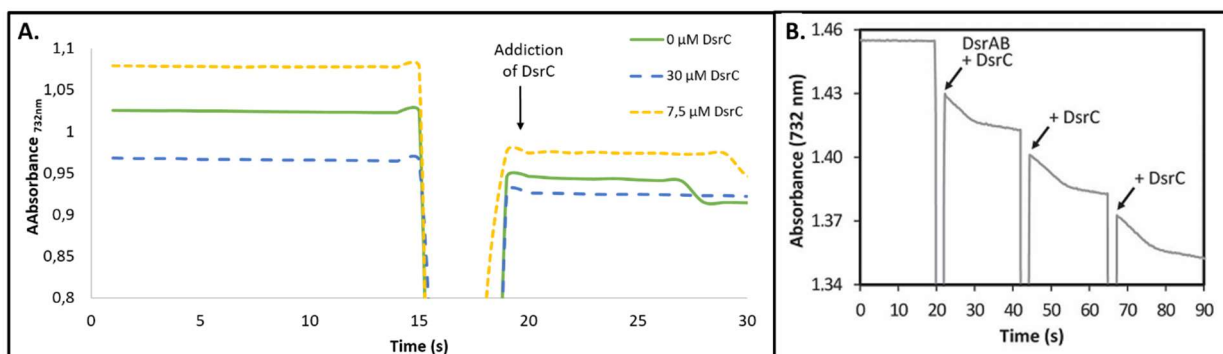


Figure III.12 – A) Kinetic results from the addition of DvH DsrC to DsrAB enzyme; B) Kinetic profile from the addition of *A. fulgidus* DsrC to DsrAB in sulfite reduction, taken from [35].

The resulting profile obtained for DsrAB and DsrC from DvH showed that when the DsrC is added to the reaction there is no significant alteration in the slope measured for the sulfite reduction, so it does not increase the activity. DsrC_C26A and DsrAB from DvH do not show any evidence of the production of the trisulfide state. However, since the rate of sulfite reduction is so low, no definitive conclusions can be drawn at this point.

The redox state of DsrC after reaction with DsrAB was analyzed with the MalPEG assay. MalPEG is a compound that binds to thiol groups of the protein, like cysteines residues, leading to an increase of the expected protein mass. If the cysteines of DsrC are reduced, they will bind to MalPEG and there is a shift in the expected mass of the protein of 10 kDa for each cysteine bound to a MalPEG molecule. According to Santos and co-authors, the cysteines of DsrC bind the sulfite-derived sulfur after reduction of sulfite by DsrAB, and in this case, there would be no shift in DsrC molecular mass because the cysteines are in oxidized state. In this study, the same approach was used to study the redox state of DsrC cysteines.

The points were taken at 0, 5 and 15 minutes after the addition of DsrC to sulfite and DsrAB. The negative control was the reduced DsrC incubated with MalPEG so that we could ensure that the protein had the two catalytic cysteines available.

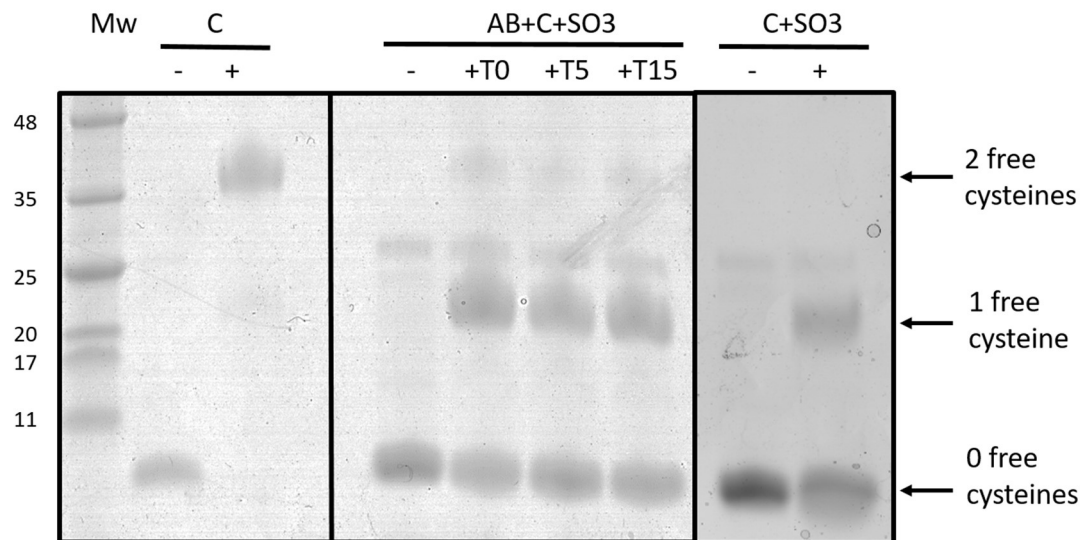


Figure III.13 - MalPEG assay; on the left panel reduced DsrC incubated (+) and non-incubated (-) with MalPEG; on the middle panel DsrC with DsrAB and sulfite non incubated (-) and incubated (+) with MalPEG at different time points during the kinetic assay, from 0 to 15 minutes (+T); on the right panel reduced DsrC after the addition of sulfite incubated (+) and non-incubated (-) with MalPEG.

In the Tricine Gels (figure III.13) we can see that after the reaction with DsrAB and sulfite DsrC produces two major bands, one without shift and another one with a shift corresponding to one MalPEG bound-cysteine. The band without shift, which could correspond to the DsrC trisulfide, appears already at T0 even before sulfite reduction. Thus, this result does not fit with being a DsrC trisulfide. Another option would be that DsrC has the capacity to bind sulfite to the free cysteines, and if so this would prevent the binding of MalPEG. This hypothesis was confirmed by incubating DsrC with sulfite, in the absence of DsrAB, and the same results were observed.

It is also possible to see that sulfite binds almost instantly to DsrC, even in the absence of the enzyme, which did not occur in the *A. fulgidus* protein [35]. The fact that DvH DsrC binds sulfite in vitro without any influence of DsrAB probably explains why the sulfite reduction rate observed was so low. In *A. fulgidus* this effect was not observed so the sulfite and DsrC were free as substrates to react with the enzyme giving rise to the DsrC trisulfide.

Further studies are required to optimize the activity of DvH DsrAB before more experiments with DsrC can be performed. Nevertheless, the observation that DsrC from DvH can bind sulfite is interesting and deserves further studies.

IV. Conclusions

Studying the role of DsrD in the dissimilatory sulfite reduction step is very important to better understand the mechanism of this process. In this thesis, most of the biochemistry assays were conducted for this purpose.

Despite the efforts to understand the function of the DsrD protein, no major conclusion was achieved. The EMSA assays showed no evidence that DsrD was able to bind DNA even with high ratios of protein versus DNA. From Far-Western blot analysis it seems that DsrD has no relevant interaction with the other Dsr proteins tested, namely DsrAB, DsrC and the membrane complex DsrMKJOP. Finally, the Thermofluor assay results showed that the stability of DsrD was not affected by sulfite or sulfide molecules, as none of them altered the melting temperature of the protein. The results obtained in this thesis do not rule out the hypothesis that DsrD interacts with DNA and/or Dsr proteins. They only show that with the techniques used it was not possible to obtain positive results. Other more sensitive techniques should be employed to study the function of DsrD.

The DsrABDC from *B. wadsworthia* was successfully purified but in terms of enzymatic characterization the enzyme showed a quite low K_m compared with other sulfite reductases. Determination of the crystal structure of DsrABDC will allow to see the conformational differences of this protein relative to the DvH DsrABC. One of the possibilities is that this protein can induce conformational changes in the DsrAB making the sulfite reduction more efficient.

The DsrAB from DvH did not show sulfite reductase activity in the presence of DsrC in any of the conditions tested. The MAL-PEG assays and a control experiment in the absence of DsrAB indicate that DvH DsrC binds one and two molecules of sulfite, which can explain the lack of activity measured for DsrAB. Since the protein did not show enzymatic activity, no other experiences using this enzyme could be performed, such as the addition of DsrD to understand if it had some effect in the process.

V. Bibliography

1. Power SE, O'Toole PW, Stanton C, et al (2014) Intestinal microbiota, diet and health. *Br J Nutr* 111:387–402. doi: 10.1017/S0007114513002560
2. O'Toole PW, Claesson MJ (2010) Gut microbiota: Changes throughout the lifespan from infancy to elderly. *Int Dairy J* 20:281–291. doi: 10.1016/j.idairyj.2009.11.010
3. Yoshioka H, Iseki K, Fujita K (1983) Development and differences of intestinal flora in the neonatal period in breast-fed and bottle-fed infants. *Pediatrics* 72:317–321.
4. Penders J, Thijs C, Vink C, et al (2006) Factors Influencing the Composition of the Intestinal Microbiota in Early Infancy. *Pediatrics* 118:511–521. doi: 10.1542/peds.2005-2824
5. Lupp C, Finlay BB (2005) Intestinal microbiota. *Curr Biol* 15:R235–R236. doi: 10.1016/j.cub.2005.03.032
6. Marchesi JR (2011) Human distal gut microbiome. *Environ Microbiol* 13:3088–3102. doi: 10.1111/j.1462-2920.2011.02574.x
7. Balzola F, Bernstein C, Ho GT, Lees C (2010) A human gut microbial gene catalogue established by metagenomic sequencing: Commentary. *Inflamm Bowel Dis Monit* 11:28. doi: 10.1038/nature08821
8. Eckburg PB, Bik EM, Bernstein CN, et al (2005) Diversity of the human intestinal microbial flora. *Science* 308:1635–8. doi: 10.1126/science.1110591
9. Ottman N, Smidt H, de Vos WM, Belzer C (2012) The function of our microbiota: who is out there and what do they do? *Front Cell Infect Microbiol* 2:1–11. doi: 10.3389/fcimb.2012.00104
10. Sommer F, Bäckhed F (2013) The gut microbiota--masters of host development and physiology. *Nat Rev Microbiol* 11:227–38. doi: 10.1038/nrmicro2974
11. den Besten G, van Eunen K, Groen AK, et al (2013) The role of short-chain fatty acids in the interplay between diet, gut microbiota, and host energy metabolism. *J Lipid Res* 54:2325–2340. doi: 10.1194/jlr.R036012
12. Flint HJ, Scott KP, Duncan SH, et al (2012) Microbial degradation of complex carbohydrates in the gut. *Gut Microbes* 3:289–306. doi: 10.4161/gmic.19897
13. Fava F, Danese S (2011) Intestinal microbiota in inflammatory bowel disease: Friend or foe? *World J Gastroenterol* 17:557–566. doi: 10.3748/wjg.v17.i5.557
14. Abraham C, Cho JH (2009) Inflammatory Bowel Disease. *N Engl J Med* 2066–2078. doi: 10.1056/NEJMra0804647
15. Brown SJ, Mayer L (2007) The immune response in inflammatory bowel disease. *Am J Gastroenterol* 102:2058–2069. doi: 10.1111/j.1572-0241.2007.01343.x

16. Maynard CL, Elson CO, Hatton RD, Weaver CT (2015) Reciprocal Interactions of the Intestinal Microbiota and Immune System. *HHS* 489:231–241. doi: 10.1038/nature11551.Reciprocal
17. Grein F, Ramos AR, Venceslau SS, Pereira IAC (2013) Unifying concepts in anaerobic respiration: Insights from dissimilatory sulfur metabolism. *Biochim Biophys Acta - Bioenerg* 1827:145–160. doi: 10.1016/j.bbabi.2012.09.001
18. Weissgerber T, Zigann R, Bruce D, et al (2011) Complete genome sequence of *Allochromatium vinosum* DSM 180(T). *Stand Genomic Sci* 5:311–330. doi: 10.4056/sigs.2335270
19. Rabus R, Venceslau SS, Wöhlbrand L, et al (2015) A Post-Genomic View of the Ecophysiology, Catabolism and Biotechnological Relevance of Sulphate-Reducing Prokaryotes. *Adv Microb Physiol* 66:55–321. doi: 10.1016/bs.ampbs.2015.05.002
20. Muyzer G, Stams AJM (2008) The ecology and biotechnology of sulphate-reducing bacteria. *Nat Rev Microbiol* 6:441–454. doi: 10.1038/nrmicro1892
21. Barton LL, Fauque GD (2009) Biochemistry, physiology and biotechnology of sulfate-reducing bacteria. *Adv Appl Microbiol* 68:41–98. doi: 10.1016/S0065-2164(09)01202-7
22. Martins M, Mourato C, Sanches S, et al (2017) Biogenic platinum and palladium nanoparticles as new catalysts for the removal of pharmaceutical compounds. *Water Res* 108:160–168. doi: 10.1016/j.watres.2016.10.071
23. Nava GM, Carbonero F, Croix JA, et al (2012) Abundance and diversity of mucosa-associated hydrogenotrophic microbes in the healthy human colon. *ISME J* 6:57–70.
24. Guo F, Yu T, Hong J, Fang J (2016) Emerging Roles of Hydrogen Sulfide in Inflammatory and Neoplastic Colonic Diseases. 7:1–8. doi: 10.3389/fphys.2016.00156
25. Bak F, Pfennig N (1987) Chemolithotrophic growth of *Desulfovibrio sulfodismutans* sp. nov. by disproportionation of inorganic sulfur compounds. *Arch Microbiol* 147:184–189. doi: 10.1007/BF00415282
26. Tanimoto Y, Bak F (1994) Anaerobic degradation of methylmercaptan and dimethyl sulfide by newly isolated thermophilic sulfate-reducing bacteria. *Appl Environ Microbiol* 60:2450–2455.
27. Heidelberg JF, Seshadri R, Haveman SA, et al (2004) The genome sequence of the anaerobic, sulfate-reducing bacterium *Desulfovibrio vulgaris* Hildenborough. *Nat Biotechnol* 22:554–559. doi: 10.1038/nbt959
28. Lovley DR, Phillips EJP (1994) Reduction of chromate by *Desulfovibrio vulgaris* and its c3 cytochrome. *Appl Environ Microbiol* 60:726–728.
29. Baron EJ, Summanen P, Downes J, et al (1989) *Bilophila wadsworthia*, gen. nov. and sp. nov., a unique gram-negative anaerobic rod recovered from appendicitis specimens and human faeces. *J Gen Microbiol* 135:3405–3411. doi: 10.1099/00221287-135-12-3405
30. Laue H, Denger K, Cook AM (1997) Taurine reduction in anaerobic respiration of *Bilophila wadsworthia* RZATAU. *Appl Environ Microbiol* 63:2016–2021.

31. Keller KL, Wall JD (2011) Genetics and molecular biology of the electron flow for sulfate respiration in *Desulfovibrio*. *Front Microbiol* 2:1–17. doi: 10.3389/fmicb.2011.00135
32. Pires RH, Venceslau SS, Morais F, et al (2006) Characterization of the *Desulfovibrio desulfuricans* ATCC 27774 DsrMKJOP complex - A membrane-bound redox complex involved in the sulfate respiratory pathway. *Biochemistry* 45:249–262. doi: 10.1021/bi0515265
33. Pires RH, Lourenço AI, Morais F, et al (2003) A novel membrane-bound respiratory complex from *Desulfovibrio desulfuricans* ATCC 27774. *Biochim Biophys Acta - Bioenerg* 1605:67–82. doi: 10.1016/S0005-2728(03)00065-3
34. Ramos AR, Keller KL, Wall JD, Cardoso Pereira IA (2012) The membrane qmoABC complex interacts directly with the dissimilatory adenosine 5'-phosphosulfate reductase in sulfate reducing bacteria. *Front Microbiol*. doi: 10.3389/fmicb.2012.00137
35. Santos AA, Venceslau SS, Grein F, et al (2015) A protein trisulfide couples dissimilatory sulfate reduction to energy conservation. *Science* (80-) 350:1541–1545. doi: 10.1126/science.aad3558
36. Schiffer A, Parey K, Warkentin E, et al (2008) Structure of the Dissimilatory Sulfite Reductase from the Hyperthermophilic Archaeon *Archaeoglobus fulgidus*. *J Mol Biol* 379:1063–1074. doi: 10.1016/j.jmb.2008.04.027
37. Oliveira F, Vonnrhein C, Matias PM, et al (2008) The Crystal Structure of *Desulfovibrio vulgaris* Dissimilatory Sulfite Reductase Bound to DsrC Provides Novel Insights into the Mechanism of Sulfate Respiration * □. 283:34141–34149. doi: 10.1074/jbc.M805643200
38. Venceslau SS, Cort JR, Baker ES, et al (2013) Redox states of *desulfovibrio vulgaris* dsrC, a key protein in dissimilatory sulfite reduction. *Biochem Biophys Res Commun* 441:732–736. doi: 10.1016/j.bbrc.2013.10.116
39. Venceslau SS, Stockdreher Y, Dahl C, Pereira IAC (2014) The “bacterial heterodisulfide” DsrC is a key protein in dissimilatory sulfur metabolism. *Biochim Biophys Acta - Bioenerg* 1837:1148–1164. doi: 10.1016/j.bbabi.2014.03.007
40. Karkhoff-Schweizer RR, Huber DPW, Voordouw G (1995) Conservation of the genes for dissimilatory sulfite reductase from *Desulfovibrio vulgaris* and *Archaeoglobus fulgidus* allows their detection by PCR. *Appl Environ Microbiol* 61:290–296.
41. Laue H, Friedrich M, Ruff J, Cook AM (2001) Dissimilatory sulfite reductase (*Desulfovibrio*) of the taurine-degrading, non-sulfate-reducing bacterium *Bilophila wadsworthia* RZATAU contains a fused DsrB-DsrD subunit. *J Bacteriol* 183:1727–1733. doi: 10.1128/JB.183.5.1727-1733.2001
42. Hittel DS, Voordouw G (2000) Overexpression, purification and immunodetection of DsrD from *Desulfovibrio vulgaris* Hildenborough. *Antonie van Leeuwenhoek, Int J Gen Mol Microbiol* 77:271–280. doi: 10.1023/A:1002449227469
43. Mizuno N, Voordouw G, Miki K, et al (2003) Crystal structure of dissimilatory sulfite reductase D (DsrD) protein - Possible interaction with B- and Z-DNA by its winged-helix motif. *Structure* 11:1133–1140. doi: 10.1016/S0969-2126(03)00156-4

44. Nicholls A, Sharp KA, Honig B (1991) Protein folding and association: Insights from the interfacial and thermodynamic properties of hydrocarbons. *Proteins Struct Funct Bioinforma* 11:281–296. doi: 10.1002/prot.340110407
45. Zhang L, Nie X, Ravcheev DA, et al (2014) Redox-responsive repressor rex modulates alcohol production and oxidative stress tolerance in *Clostridium acetobutylicum*. *J Bacteriol* 196:3949–3963. doi: 10.1128/JB.02037-14
46. Grimm F, Dobler N, Dahl C (2010) Regulation of *dsr* genes encoding proteins responsible for the oxidation of stored sulfur in *Allochromatium vinosum*. *Microbiology* 156:764–773. doi: 10.1099/mic.0.034645-0
47. Mancini S, Kumar R, Abicht HK, et al (2016) Copper resistance and its regulation in the sulfate-reducing bacterium *desulfosporosinus* sp. OT. *Microbiol (United Kingdom)* 162:684–693. doi: 10.1099/mic.0.000256
48. Leavitt WD, Bradley AS, Santos AA, et al (2015) Sulfur isotope effects of dissimilatory sulfite reductase. *Front Microbiol*. doi: 10.3389/fmicb.2015.01392

Supplementary Data

Table S.1 – Growth medium for *Desulfovibrio vulgaris* Hildenborough.

Component	Final Concentration
MgCl ₂	8 mM
NH ₄ Cl	20 mM
CaCl ₂	0.6 mM
K ₂ HPO ₄ -NaH ₂ PO ₄	2 mM
Trace elements*	
FeCl ₂	0.06 mM
EDTA	0.12 mM
Tris-HCl pH 7.4	30 mM
Thauers Vitamins**	

* ZnCl₂, MnCl₂·4H₂O, H₃BO₃, CoCl₂·4H₂O, CuCl₂·2 H₂O, NiSO₄·6H₂O, Na₂MoO₄·4H₂O, Na₂SeO₃·5 H₂O, Na₂WO₄·2H₂O

**Biotin, Acid folic, pyridoxine HCl, thiamine HCl, Riboflavin, Nicotinic Acid, DL pantothenic acid, p-aminobenzoic acid, lipoic acid, choline chloride, vitamin B12

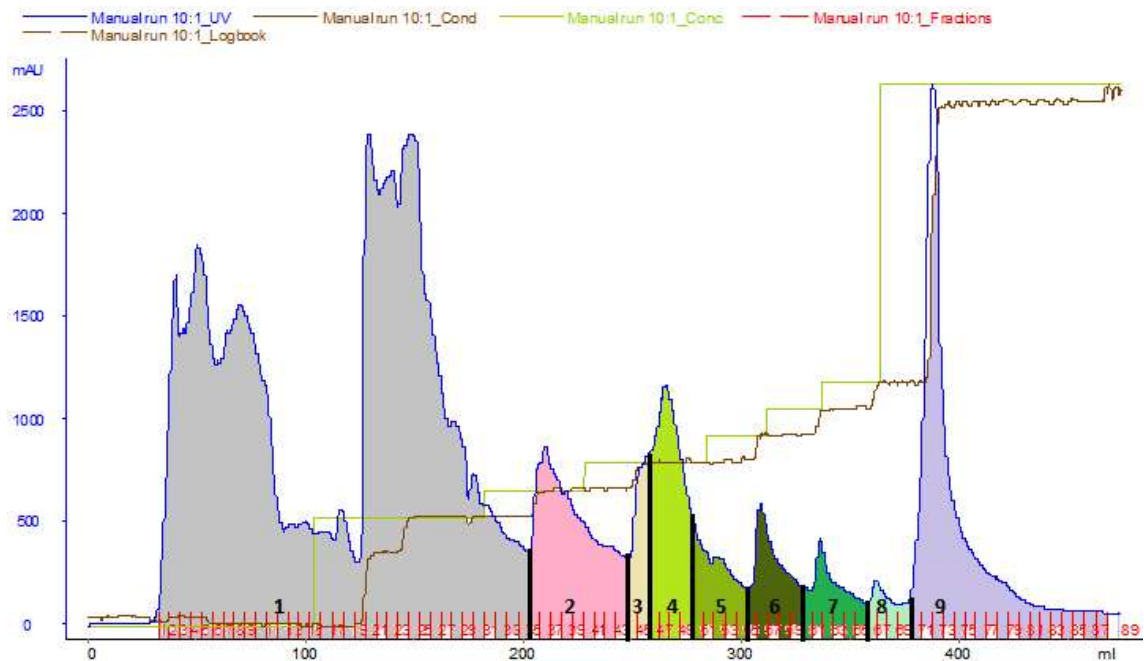


Figure S.2 – Chromatogram from Q-Sepharose column for the purification of *DsrABDC* from *Bilophila wadsworthia*.

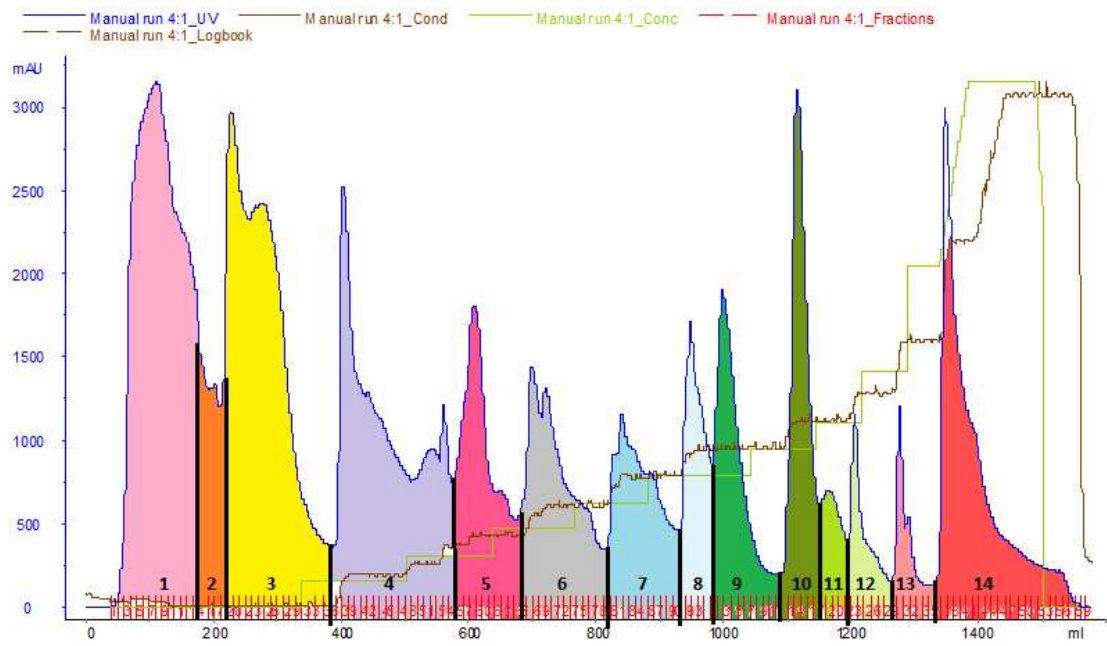


Figure S.2 – Chromatogram from Q-Sepharose column for the purification of DsrABC from DvH.